Conference Paper, Published Version

Muste, Marian; Yu, K.; Fujita, Ichiro

Traditional versus Two-Phase Perspective on Turbulent Channel Flows with Suspended Sediment (Vergleich von traditioneller und auf Zweiphasenströmung basierender Betrachtung turbulenter Gerinneströmungen mit Schwebstofffracht)

18 Traditional versus Two-Phase Perspective on Turbulent Channel Flows with Suspended Sediment

Vergleich von traditioneller und auf Zweiphasenströmung basierender Betrachtung turbulenter Gerinneströmungen mit Schwebstofffracht

M. Muste & K. Yu

IIHR-Hydroscience & Engineering, The University of Iowa, U.S.A.Engineering
IIHR-Wasser- & Ingenieurwissenschaften, Universität Iowa, U.S.A.

I. Fujita

Kobe University, Japan
Universität Kobe, Japan

ABSTRACT: The present paper provides new insights into sediment-laden flows using two-phase experimental investigations facilitated by image velocimetry techniques. Two series of flume experiments with increasing concentration of buoyant and neutrally-buoyant sediment fully suspended in a turbulent open channel flow are reported. The results illustrate that the suspended particles affect the underlying turbulent channel flow throughout the depth irrespective of their inertia. Comparison of the results obtained for the two particle types reveals the effect of the particle inertia on the horizontal and vertical velocity lag between water and particles in the mixture, changes in flow turbulence, eddy viscosity, and sediment concentration. As expected, particle inertia mostly affects the vertical turbulence intensities and the increase in the sediment concentration better substantiates the change trends. Particle turbulence intensities in the present experiments are larger than those of the fluid throughout the outer region revealing a significant momentum exchange between the phases.

KURZFASSUNG: Der vorliegende Beitrag stellt neue Erkenntnisse zur sedimentbelasteten Stömung vor, die in einer zweiphasigen Modellierung experimentell mit unterstützender Hilfe der Bildverarbeitungstechnik ermittelt wurden. Über zwei Laborgerinneexperimente mit turbulenter Gerinneströmung wird berichtet, die sich mit teilweise und vollständig ausgebildeter Geschiebefracht beschäftigen. Die Resultate veranschaulichen den Einfluss von vollständig suspendierten Geschiebeteilchen auf die darunter befindliche turbulente Gerinneströmung, den diese über die gesamte Wassertiefe unbeeinflusst von der Teilchenträgheit ausüben. Der Vergleich der Ergebnisse, die mit zwei unterschiedlichen Teilchentypen erhalten wurden, zeigt keinen Unterschied hinsichtlich des Einflusses der Teilchenträgheit auf die horizontalen und vertikalen Geschwindigkeitsdefizite der schwebstoffbefrachteten Strömung, auf die Änderung von Strömungsturbulenz, Wirbelviskosität und Sedimentdichte. Wie zu erwarten war, hat die Teilchenträgheit auf die vertikale Turbulenzintensität und auf das Anwachsen der Sedimentkonzentration Einfluss, was sich deutlich in den tendenziellen Veränderungen abbildet. In den vorliegenden Ergebnissen sind die Intensitäten der Teilchenturbulenzen größer als die der benachbarten Strömungsregionen, was darauf hindeutet, dass ein signifikanter Impulsaustausch zwischen beiden Phasen stattfindet.

1.1 Introduction

Suspended sediment is distributed over most of the flow depth and has larger downstream velocities than sediment moving near the bed, therefore the total sediment load in rivers is often dominated by the suspended load. Since the role of fine sediment on the environment has only been recently understood, there is an immediate need for in-depth investigation of the spatially and temporally varying processes that suspend, transport, and deposit sediment. Suspended-sediment transport comprises an especially complex two-phase flow. Even for its simpler case in uniform open-channel flow, suspended sediment transport includes difficulties attributable to sediment concentration and velocity gradients across the flow depth, non-homogeneous channel turbulence, the irregularity of sediment particle shape, simultaneous presence of a range of particle sizes, and the multiple interactions between the two flow phases.

Extensive research efforts in the last few decades have only partially elucidated the complexities of suspended-sediment transport. Lacking adequate formulation and quantification of the interaction between suspended particles and the carrier liquid, it is common practice to combine the available sediment mechanics theory and empiricism to obtain predictive formulations for suspended sediment transport. Raudkivi (1999) has recently remarked that the available theories are quite limited and more research should be oriented toward understanding and formulation of the physical processes involved in these flows. The understanding effort is timely, because there is an increased tendency to solve suspended sediment transport problems using numerical models, despite that considerable questions are raised on the quality of physical relationships on which these models are based.

The new generation of nonintrusive instruments now facilitates further understanding of channel flows carrying suspended sediment. Increasingly powerful such techniques allowed documentation of the near wall coherent structures and their higher level of self-oganization leading persistent alternative low- and high-speed velocity streaks (e.g., Sumer & Oguz 1978; Sumer & Deigaard 1981; Rashidi et al. 1990, Wei & Willmarth, 1990; Soulsby, 1994, Nino & Garcia, 1996). Among other insights, the new investigative tools undoubtedly revealed a measurable velocity lag between the streamwise fluid and sediment velocities and a variation of its magnitude both with the depth and sediment concentration (Kaftori et al., 1995; Muste, 1995: Taniere et al., 1997; and Kiger & Pan, 2002). Additionally, studies have shown that the underlying flow turbulence is attenuated or enhanced by suspended particles in an intricate relationship with several sediment-flow parameters (e.g., Tsuji & Morikawa, 1982; Elghobashi & Abou-Arab, 1983; Rashidi et al., 1990; Gore & Crowe, 1991; Rogers & Eaton, 1991; Yarin & Hetsroni, 1994). Despite these initial findings, there is a growing awareness within the scientific community that the sediment research area is stagnating and there is an imperious need for a better understanding of the fundamentals of the processes involved. Recent specialized meetings, such as Erosion and Sediment Transport Measurement: Technological and Methodological Advances (Oslo, Norway, 2002) and Sedimentation and Sediment Transport: at the Cross Roads between Physics and Engineering (Monte Verita, Switzerland, 2002) are illustrative examples of searching efforts aimed at surpassing the status quo. The multitude of parameters involved and their unknown interaction preclude at this time prediction of the changes produced by the sediment on the carrier flow even in the simplest sediment laden-flows. Current efforts are directed toward critical review of the knowledge status, call for new approaches, new strategies, and new methods for developing an improved understanding of the cause-effect relationship in sediment-water interaction (Sherwood et al., 2003; Hanratty et al., 2003; Sundaresan et al., 2003).

Today's principal scientific issue regarding sediment-laden flows is the understanding of why the phases configure in a certain way (Hanratty et al., 2003) and subsequent development and validation of models that integrate the correct microphysics in appropriate averaged equations. The formulation of these later equations presents challenges since the structure of the phase distribution could affect the choice of averaging methods and closure relations. The solution to this problem involves the discovery of the small-scale interactions between the phases that are controlling the macroscopic behavior of the multiphase flows through complementary laboratory and numerical experiments. It is obvious, however, that the description of this finer detail of the flow cannot be accomplished without using two-phase investigative tools, models or experimental techniques capable of discriminating the plow phases.

The increased level of complexity for the investigation of suspended sediment transport using the two-phase flow approach might sound overstated for engineering hydraulics. However, improvement of modeling and predictive formulation of suspended sediment transport cannot be sustained without further insights into the nature of particle–fluid and particle–particle interactions and clarification of the energy transfer between flow phases, among other needs. The findings reported in this paper attempts to provide experimental evidence aimed at providing new insights into the micro-mechanics of suspended particulate transport using two-phase experimental investigations facilitated by image velocimetry techniques.

1.2 EXPERIMENTS

1.2.1 Experimental Context

Open channel turbulent flows are characterized by the existence of persistent coherent structures, particularly in the near-wall region, that include ejections and sweeps and their higher state of organization in low- and high-speed streaks. Particle in suspension in sediment-laden flows are moving under the action of body forces and the coherent wall structures. In turn, particles are acting on the flow through two mechanisms (Kaftori et al. 1998). One is due the presence of the particles at the wall as "moving roughness" and it is similar to effect produced by stationary roughness. The second is the result of the particle-fluid structure interaction that takes place throughout the flow depth. Additional complexities occur if the concentration for the suspended fraction exceeds 10-3 when particle-particle interactions become important.

Most of the available experiments on suspended sediment transport with natural sand (specific gravity about 2.65), from the classical work of Vanoni (1946) to recent two-phase experiments, Bennett et al. (1998), Muste & Patel (1997), Best et al. (1997), Kiger & Pan (2002), Righetti & Romano (2004) have reported the existence of long, persistent sediment streaks on the channel bed formed by particle deposited in the low-speed streaks associated with the wall coherent structure. Even experiments with neutrally-buoyant particles, as those reported by Rashidi et al. (1990) and Kaftori et al. (1995.a; 1195.b, 1998) noted the streak presence. Sediment streaks materialize the low- and high-velocity streaks formed by the self-organized structures acting in the wall region. They are more prominent when particles are heavier (even if the bulk sediment concentration is in the 10-3 to 10-4 dilute concentration range) or when the bulk flow velocity in the channel low. Streak presence does not necessarily imply that the sediment is deposited on the channel bed, rather it is moving along the streak direction acting like a "moving" roughness.

The writers carried out two sets of experiments originated from clear water flows; one set with natural sand (NS), the other with neutrally-buoyant sediment (NBS), formed of crushed nylon. The particle size, shape factor, and sediment concentrations were same for the two experiment sets. A major difference between the writers' experiments and the earlier experiments is the lack of sediment streaks for the discussed experiments. The high *Fr* numbers for the NS and NBS sets confirm that writers' flows were highly turbulent with all the sediment in suspension. Consequently, the primary interaction involved in the present experiments is the particle-fluid structure one, rather that the alternative roughness-like mechanism. The insights from the previous studies complement those of the present study insofar that, for a range of particle and flow characteristics, they show the combined outcome of the two effects on flow turbulence.

1.2.2 Experiment Setup and Procedures

The experiments were focused on dilute disperse sediment in open-channel turbulent flow where the volume fraction of particles is very small and interparticle collisions limited. In such flows the two-way coupling, where the motion of the fluid has a significant effect on the particle motion and vice versa, is dominant. Consequently, the experimental design was driven by two key elements. First, the experiments with sediment were conducted such that no deposition of sediment on the bed was allowed. Without bedload transport, all the changes in the underlying flow can be attributed to the presence of suspended sediment, thus facilitating understanding of underlying mechanisms of the suspension processes and their subsequent formulation. The second key element of the experimental design was use of a two-phase flow velocity instruments that allowed separate and simultaneous non-intrusive measurements on solid and liquid phase. A combination of image velocimetry (IV) cross-correlation and particle tracking techniques has been designed and implemented to provide mean and turbulence flow characteristics in a plane.

The experiments were conducted using a tilting recirculating flume, 6.0 m long, 0.15 m wide at Kobe University, Kobe, Japan. The flume bed was made of smooth finished stainless steel with glass walls and bottom. Plastic honeycombs were set at the flume entrance to facilitate quick flow development, minimize air entrainment, and ensure flow uniformity. The volumes of the head and tail tanks were kept at minimum to avoid sediment deposition. The tanks were fitted with edge fillers to avoid sediment accumulation. Both tanks have been continuously inspected during the measurements for sediment retention. Flow depths were measured with a 0.01 mm resolution digital micrometer placed on an instrumentation carriage. The flume was covered, the room temperature kept approximately constant, and experiment conducted in full darkness to preserve the flow quality and recording conditions.

Two series of tests were conducted starting with clear (distilled) water flows (CW). The experiments were conducted at a single flow rate (maximum streamwise velocity of approximatively 1 m/s), which was selected such that the turbulence intensity would be sufficient for particle suspension maintenance. The flow depth was kept small to obtain a large channel aspect ratio (i.e., 7.5) that prevents formation of secondary flows in the channel. Sediment-laden flows were obtained by successively adding sediment to the original clear flows. Channel slope was kept at 0.0113 m/m for all tested flows. The flows were checked for flow uniformity following each sediment addition, but no measurable change in the free-surface slope was noticed using the available instrumentation. All reported measure-

ments were conducted on the flume centerline, in a test section located 5.3 m downstream the flume inlet. Preliminary velocity measurements in the streamwise and spanwise direction in the test section area documented that a fully developed uniform free-surface flow was attained.

Two kinds of sediment particles were used in the tests; natural sand (NS) and neutrally-buoyant sediment (NBS) consisting of crushed Nylon particles. The NS and NBS particles were carefully sieved within the 0.21~0.25 mm size range and were practically of similar shape irregularity. The sediment concentration for the three consecutive NS and NBS flows were identical, in the 0.0005 – 0.0015 volumetric concentrations range. Consequently, the only difference between the two sediment-laden flows was the specific gravity of the sediment, i.e., 2.65 for the natural sand and 1.02~1.03 for the crushed Nylon. As mentioned before, no sediment deposition was allowed to develop anywhere on the flume bed and in the flow circuit. No sediment streaks were observed on the channel bed during the conducted experiments. Visible streaks occurred only for the highest concentration with natural sand flow (NS3) when the velocity was lowered 20%. Tables 1 and 2 present the summary of the main sediment characteristics and experimental conditions for the tested flows. Fall velocities displayed in the tables were calculated using Dietrich's (1982) formula with the particle diameter with D_{50} = 0.23 mm and densities of 2,650 kg/m^3 and 1,025 kg/m^3 for the natural sand and neutrally sediment particles, respectively.

The imaging system used for conduct of the velocity measurements comprised illumination, image capture, and data acquisition components. Two pulsed Yag-lasers, Model ULTRA (Big Sky Laser) were used for illumination. These pulsed lasers have a nominal e^{-2} beam diameter of 2.5 mm and emit 20 mJ over 5 ns pulsewidth. The lasers were enclosed in a housing that combined and transformed the two beams into a sheet. Lasers were pulsed at 15 Hz by an electronic timing box that triggered the lasers at 0.2 msec time separation. Nylon 12 spheres of 0.02 mm and 1.02~1.03 specific gravity were used as water tracers. Distilled water was used for all experiments to enhance the image quality. Water was recirculated more than two hours before each experiment to ensure that tracers were uniformly dispersed in the flow.

Images were captured with Kodak Megaplus, ES 1.0 progressive scan camera. The timing box activates the doubled triggered exposure mode of the camera that allows for two full-frame images to be acquired within a time separation of 5 μs. The camera resolution is 1008 by 1018 pixels with each pixel measuring 9 μm square. The digital images capturing was controlled by XCAP software. Image pairs were recorded at 15 Hz and transmitted to a PC through a frame grabber board. About 6,000 image pairs were recorded and stored for each flow case. 20 series of 300 image pairs (20s per realization) were sequentially collected over about 10 minutes for each case in order to randomly sample the flow field. The time between recordings was needed for transferring the images to the computer.

Table 1. Experimental conditions for the first series of tests

Experiment		**CW1**	**NS1**	**NS2**	**NS3**
		Water	Natural sand	Natural sand	Natural sand
	Depth (m)	0.021	0.021	0.021	0.021
	Bed slope	0.0113	0.0113	0.0113	0.0113
	Temperature (°C)	22~23	23	22	23~24
Sediment	S.G.	-	2.65	2.65	2.65
	Size range (mm)	-	0.21~0.25	0.21~0.25	0.21~0.25
	Fall velocity (m/s)	-	0.024	0.024	0.024
	Vol. Conc.($\times 10^3$)	0.00	0.46	0.92	1.62

Table 2. Experimental conditions for the second series of tests

Experiment		**CW2**	**NBS1**	**NBS2**	**NBS3**
		Water	Crushed Nylon	Crushed Nylon	Crushed Nylon
	Depth (m)	0.021	0.021	0.021	0.021
	Bed slope	0.0113	0.0113	0.0113	0.0113
	Temperature (°C)	22~23	23	22	23~24
Sediment	S.G.	-	1.02~1.03	1.02~1.03	1.02~1.03
	Size range (mm)	-	0.21~0.25	0.21~0.25	0.21~0.25
	Fall velocity (m/s)	-	0.0006	0.0006	0.0006
	Vol. Conc.($\times 10^3$)	0.00	0.46	0.92	1.62

Processing of the image pairs was made with a combination of Particle Image Velocimetry (PIV) Particle Tracking Velocimetry (PTV). PIV processing is based on pattern-matching algorithms applied to images seeded with high water tracer concentrations providing regularly spaced velocity estimates. PTV tracks individual particle images and estimate their displacement by analyzing image pairs to eventually assign velocities to each of the identified particle. A novel algorithm for phase discrimination was developed for this application by Yu (2004). Phase discrimination is based on the size criterion, similar to the approach employed earlier by Muste et al. (1998). The new processing software was considerably improved to minimize crosstalk, remove

reflections produced by sediment particles located near the bed, and improve water tracer detection in the vicinity of sediment particle images.

The PIV-PTV processing was intertwined using an approach similar to that developed by Cowen & Monismith (1997). The first processing step is conducted with PIV applied to small interrogation areas to estimate the flow displacement between successive images (Yu, 2004). The second processing step uses those estimates in conjunction with PTV algorithms to estimate displacements of individual water tracers and sediment particles. The end result is an irregular vector map with considerably increased number of vectors compared to PIV applied to the same image pair. The accuracy of the develop PIV-PTV processing was tested using artificial images and imposed displacements. The processed results showed differences less than 1% from the imposed displacements over the imaged area. Flow properties and sediment distributions were obtained by analyzing the entire series of images recorded for a given flow.

Velocity and particle number statistics were calculated in a number of sampling bins stacked over the image vertical. The length of the sampling bins was same as the image length, while the heights were non-uniform. The height of the sampling boxes was gradually decreased near the bed (the smallest computational cell near the bed was y^+ = 2.5) to maximize the number of particles within each sampling bin, minimize the effect of strong gradients near the bed, and to provide increased resolution of the measured quantities near the bed. An instantaneous result was obtained as the average of all the water tracers in a sampling bin at one instant in time. Time averages of various reported quantities were obtained by further taking the mean over all realizations in a recording series (ensemble). Excepting the cases where otherwise specified, all the statistics were calculated using this procedure.

1.3 EXPERIMENTAL RESULTS

1.3.1 Streamwise Velocity Distributions for the Water-Sediment Mixture

Given that most of the available literature and current analytical formulations consider suspended sediment transport as a mixture of water and sediment, the streamwise velocity profiles of the current measurements are presented first using the conventional approach (without flow phase discrimination) to reference the current to previous results. Table 3 presents relevant flow parameters for the natural sand (NS) and neutrally-buoyant (NBS) experiments. The friction velocity values reported in Table 3 are obtained from the momentum balance equation for the channel flow using bulk flow measured quantities (u_{*1}) and based on the extrapolation of the measured Re stress (u_{*2}) toward the bed (Muste and Patel, 1997). Given the larger measurement uncertainties for the first method, the extrapolation of the Re stresses approach was retained for determining the friction velocity throughout the paper.

Using the above data reduction procedures, a systematic decrease up to 10% of the Karman coefficient with sediment concentration is observed for the NS flow cases, consistent with numerous previous investigations (e.g., Vanoni, 1946; Einstein and Chien, 1955). As expected, the depth-averaged streamwise velocity of the mixture decreases with sediment concentration. For the NBS flow cases, no notable changes are observed in the friction velocities computed with the momentum balance, while a slight decrease with concentration is observed for the friction velocities determined with the Re stress extrapolation method. A smaller reduction of Karman coefficient is also noted. The results for the NBS flow cases are in agreement with the experiments with neutrally-buoyant particles conducted by Elata & Ippen (1961), who observed no changes in resistance factor (for sediment concentrations up to 0.20%), clear decrease in km with sediment concentration, and increase of the velocity in the outer layer.

Table 3. Flow parameters of water-sediment mixture

NS experiments					
Experiment		**CW1**	**NS1**	**NS2**	**NS3**
Re		17,670	17,650	17,420	17,340
Fr		1.89	1.81	1.76	1.75
u_* (m/s)	u_{*1}	0.042	0.042	0.043	0.043
	u_{*2}	0.042	0.042	0.043	0.043
κ_m		0.402	0.396	0.389	0.367
Mean bulk velocity (m/s)	$\overline{U}_m$	0.839	0.813	0.796	0.792
NBS experiments					
Experiment		**CW2**	**NBS1**	**NBS2**	**NBS3**
Re		16,940	17,570	18,220	18,400
Fr		1.76	1.70	1.70	1.70
u_* (m/s)	u_{*1}	0.042	0.042	0.042	0.042
	u_{*2}	0.042	0.041	0.040	0.040
κ		0.402	0.392	0.387	0.373
Mean bulk velocity (m/s)	$\overline{U}_m$	0.798	0.772	0.773	0.772

Figure 1 contains average velocity profiles of the mixture for all measured flow cases along with the reference log-law velocity distributions using Nezu & Nakagawa (1993) values for the constants in the law.

The clear water flow cases show good agreement with the reference curve. A progressive reduction of the velocity magnitude similar to that produced by a rough wall is noted as the sediment concentration increases for the NS flow cases. An apparent increase of the normalized streamwise velocities can be observed in Figure 1.b. for the NBS flows cases with the increase of the sediment concentration, due to the slight decrease of the friction velocity.

The common trends shown by the NS and NBS experiments are the reduction of the mean bulk flow velocity and a reduction of k_m with concentration. Among the factors commonly associated with the alteration of the velocity profiles can be changes in the fluid viscosity and/or density (Coleman, 1986), the boundary roughness (Best et al., 1997), and momentum exchange mechanism near the bed (Umeyama and Gerritsen, 1992). The effective kinematic viscosity has been changed with less than 0.9% for both NS and NBS experiments, hence it was deemed that this effect is negligible. The change in density can be related to the Richardson number (Guo, 2001), but for the present flow conditions, similarly to previous studies (Wang & Qian, 1989; Einstein & Chien, 1955; and Bennett et al., 1998), there is not a clear trend between the reduction of k_m and the Richardson number (Yu, 2004).

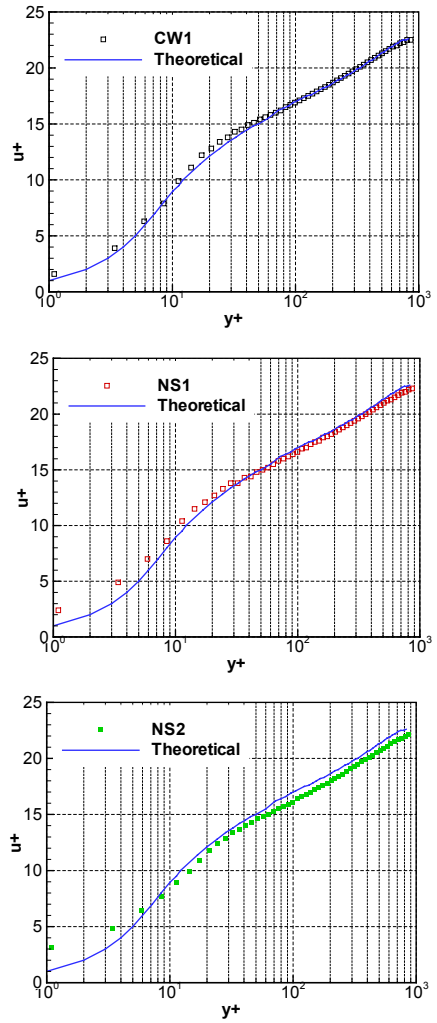

a.)

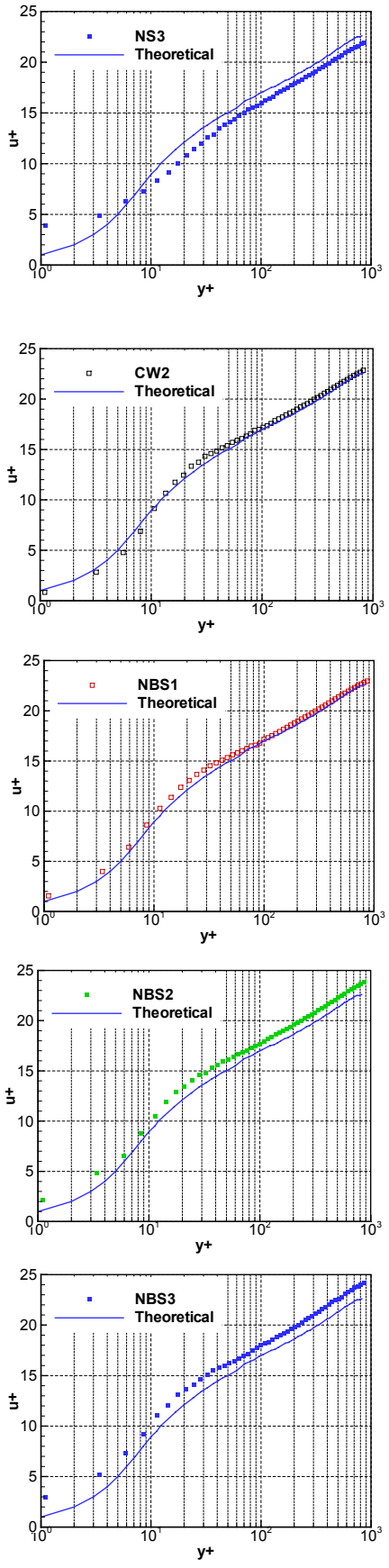

b.)

Figure 1. Streamwise velocity of water-sediment mixture: a) NB experiments; b) NBS experiments

1.3.2 Velocity Distributions for the Flow Phases

Streamwise Velocity

This section presents the mean velocity profiles using a two-phase flow investigative approach, where velocities of water tracers and sediment particles are separated and independently plotted to illustrate relevant flow physics. Table 4 summarizes selected water and sediment hydrodynamic characteristics for the NS and NBS flow cases. Subscripts "w" and "s" are for water and the sediment, respectively.

Table 4. Hydrodynamic characteristics for water and sediment

NS experiments					
Experiment		CW1	NS1	NS2	NS3
u* (m/s)	u_{*1}	0.042	0.042	0.043	0.043
	u_{*2}	0.042	0.042	0.042	0.042
κ_w		0.402	0.402	0.380	0.374
Mean bulk velocity (m/s)	$\overline{U}_w$	0.839	0.813 (-3.1%)	0.796 (-5.1%)	0.793 (-5.5%)
	$\overline{U}_s$	-	0.786	0.758	0.753
NBS experiments					
Experiment		CW2	NBS1	NBS2	NBS3
u* (m/s)	u_{*1}	0.042	0.042	0.042	0.042
	u_{*2}	0.042	0.041	0.040	0.040
κ_w		0.402	0.405	0.398	0.384
Mean bulk velocity (m/s)	$\overline{U}_w$	0.798	0.777 (-2.6%)	0.773 (-3.1%)	0.788 (-1.3%)
	$\overline{U}_s$	-	0.769	0.769	0.777

Comparison of Tables 3 and 4 illustrates that the friction velocities determined from the distribution of the Reynolds stress for water (rather than the mixture) are practically not changed with sediment addition. Despite that the friction velocities such determined are not changed, it can be noted that the bulk flow velocity is gradually reduced when sediment is added to the successive flows for both NS and NBS flow cases, as illustrated by Figures 1.a and 1.b, respectively. The Karman coefficient for water velocity profiles in the sediment-laden flows for both particle types is consistently smaller than that of the mixture and its decrease is proportional to sediment concentration. It can be noted that up to volumetric concentrations of 10^{-3}, the Karman coefficient is practically unchanged. The observation is consistent with previous results obtained by Muste & Patel (1997) where the sediment concentration for similar experiments was of the order of 10^{-4}.

Figure 2.a presents separately the streamwise velocity profiles for water and sediment particles for the NS flow cases. Water velocity profiles are gradually decreased compared with the reference clear water flow, a trend that is more evident with the increase of sediment concentration. It is apparent that particle velocity profiles are "lagging" the water profiles throughout the overlap and the outer regions. Table 4 shows that the bulk flow velocities for sediment particles are up to 4~5 % slower than those for water for the most of the water depth. Measurements shows that in the near-bottom region, for $y^+ < 10$, sediment velocities are larger than water velocities. The changes in the outer flow are by now quite common (e.g, Muste & Patel, 1997; Kiger & Pan, 2002). The changes near the wall were documented only recently by Kulick et al. (1994), Righetti & Romano (2004) using two-phase flow measurements with Laser Doppler Velocimeters (LDV) and by Kiger & Pan (2002) with PIV-PTV.

Figure 2.b. contains plots of streamwise velocity profiles separated according to the flow phase for the NBS cases. The major difference compared with the NS velocity profiles is a much decreased velocity lag between sediment and water, suggesting that the lag is mostly associated with particle inertia. Velocity profiles in Figure 2.b. are similar to those obtained with LDV measurements by Kaftori et al. (1998) for flows laden with particles in the 100-900 μm size range and volumetric concentration of about 10^{-4}. The experiments of Sumer & Deigaard (1981) and Rashidi et al. (1990) conducted with neutrally particles showed, however, that the velocity difference increases with the increase of the particle size.

The slight decrease in the water average streamwise velocity profiles observed in Figure 2.a for the NS flow cases without a change in the friction velocity might surprise because most of the previous observations made on dilute sediment-laden flows with volumetric concentrations in the 10^{-3} to 10^{-4} range showed an increase of the friction velocity with the addition of sediment (Muste & Patel, 1997; Kiger & Pan, 2002; and Righetti & Romano, 2004). The later studies noted visible long sediment structures (streaks) along the bed. The same was observed by Best et al. (1997), Bennett et al. (1998), Graf & Cellino (2002) in their experiments conducted with a continuous (moving or fixed) sediment layer on the bed. These later studies showed not only an increase of the friction velocity compared with the "reference" clear water flow but a proportional increase with sediment concentration. Reminding that for the present experiments with practically same bulk flow concentrations there was no sediment depositions or streaks in the flume, the observed decrease of the velocity profiles when the heavy sediment was added cannot be related to the bed "roughness", rather suggests that the interaction between the par-

ticle and turbulent coherent structures produces this change. This conclusion is also supported by Lyn's (1991) results, who found that for the lower concentrations of sediment ("starved-bed" flows series) the friction velocities were essentially unchanged, while for higher sediment concentrations, yet in the dilute range, increase of the friction velocity up to 20% and a correspondingslow down of the water the velocity profile was found.

The velocity lag between water and particles requires some conceptual clarification. It is obvious that there could not be an actual slip between water and sediment particles in their instantaneous interaction because that would violate the no-slip condition acting on the fluid boundaries (here played by sediment particles). Without local slip velocity, the outstanding explanation for the average velocity lag in the streamwise direction can be explained by the tendency of the sediment particles to reside in the flow structures moving with lower velocities (Summer & Deigaard, 1981; Kaftori et al., 1995.b; Kiger & Pan, 2002). The intriguing inverse lag near the bed stems from the fact that sediment particles are not bounded by viscosity shear as fluid particle are, hence the no-slip condition at the channel bottom does not apply for the sediment velocity profile.

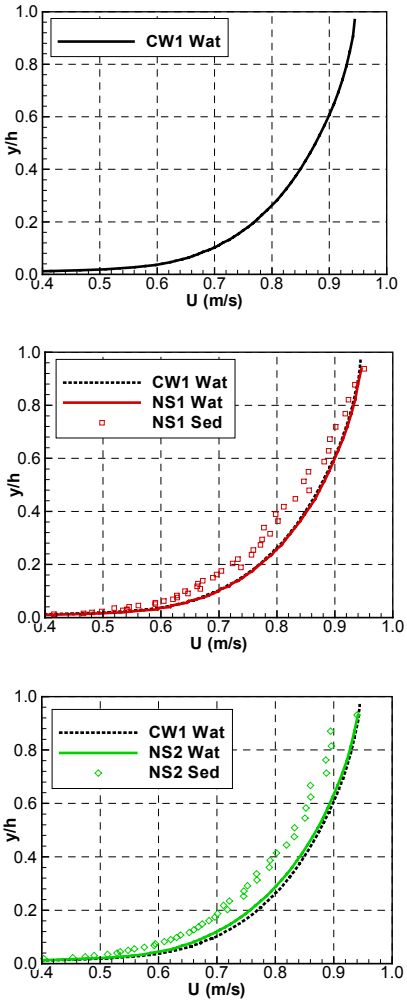

a.)

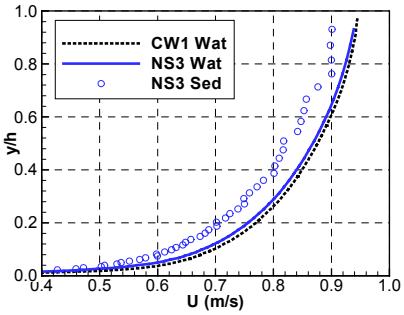

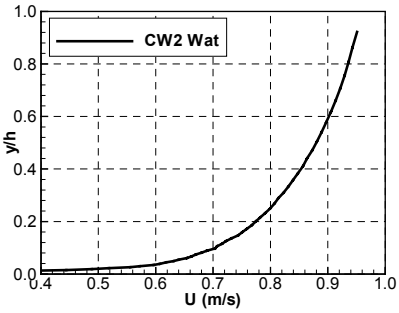

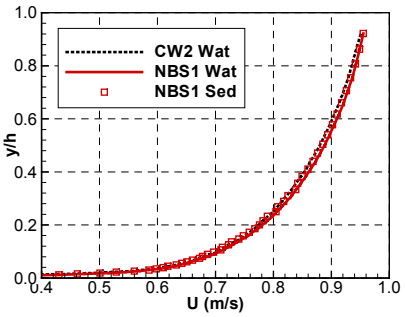

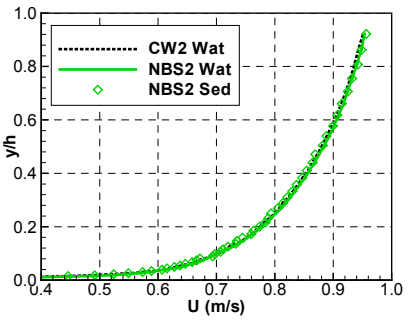

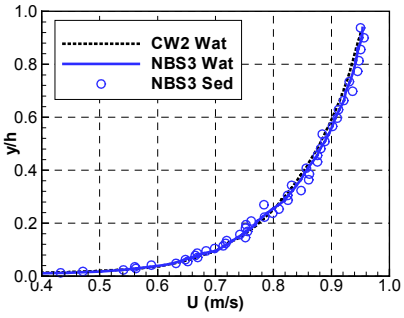

b.)

Figure 2. Streamwise velocity for water and sediment particles: a) NS experiments: b) NBS experiments

Figure 3 plots the depth distribution of the lag between water and sediment particles for the NS flow cases. These plots confirm the previous results of Sumer & Deigaard (1981), Rashidi et al. (1990), Wang & Ni (1991), and Muste & Patel (1997) indicating that the lag is larger near the bottom. Figure 3 includes the velocity lag distribution obtained with Greimann et al. (1999) formulation

$$u_G = v_s\, 0.66(1-\eta)^2 \exp(1.34\eta) \qquad (1)$$

where u_G is the Greimann's velocity lag magnitude, η is the dimensionless height ($= y/h$) and v_s is the sediment settling velocity. The plots reveal that sediment concentration increases the lag and its distribution over the depth and needs to be incorporated in the correlation.

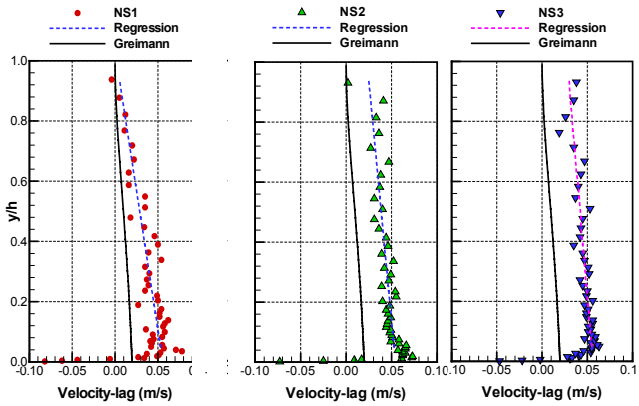

Figure 3. Distribution of the water-sediment velocity-lag for NS experiments

Vertical Velocity

A notable feature of the present results is the distribution of the vertical velocity distributions. Figure 4.a shows vertical velocity distributions for the NS experiments obtained by calculating the conventional time average of the vertical velocities for water and sediment using the available measurement samples. As expected, the average vertical velocity of water is very close to zero while sediment particle vertical velocity distributions display a considerable upward shift of the mean velocity. More insights into this apparently conflicting particle hydrodynamics is illustrated in Figure 4.b, where the vertical velocity profiles for water and sediment particles are split according to their direction of movement on the vertical; i.e., upward and downward. It can be noted that the upward and downward vertical velocity profiles for water are quasi symmetric around the vertical axis, but not constant in magnitude. Toward the bed (for $y/h < 0.3$) both velocity profiles increase in magnitude and abruptly decrease near the bed. For all flow cases, and more evident for the clear-water case, the upward average velocity profiles exceed the downward one. Results similar to those reported in Figure 4.b for sediment were also found by Bouvard & Petkovic (1985), Wei & Willmarth (1991), Kiger & Pan (2000), and Wang (2000).

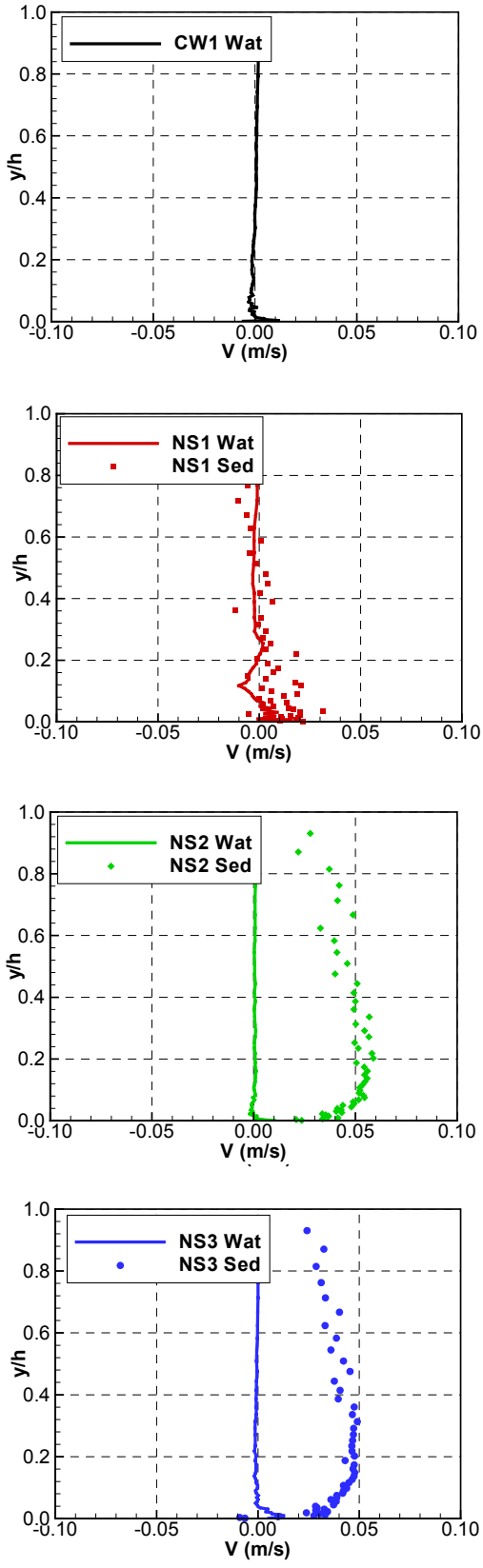

a.)

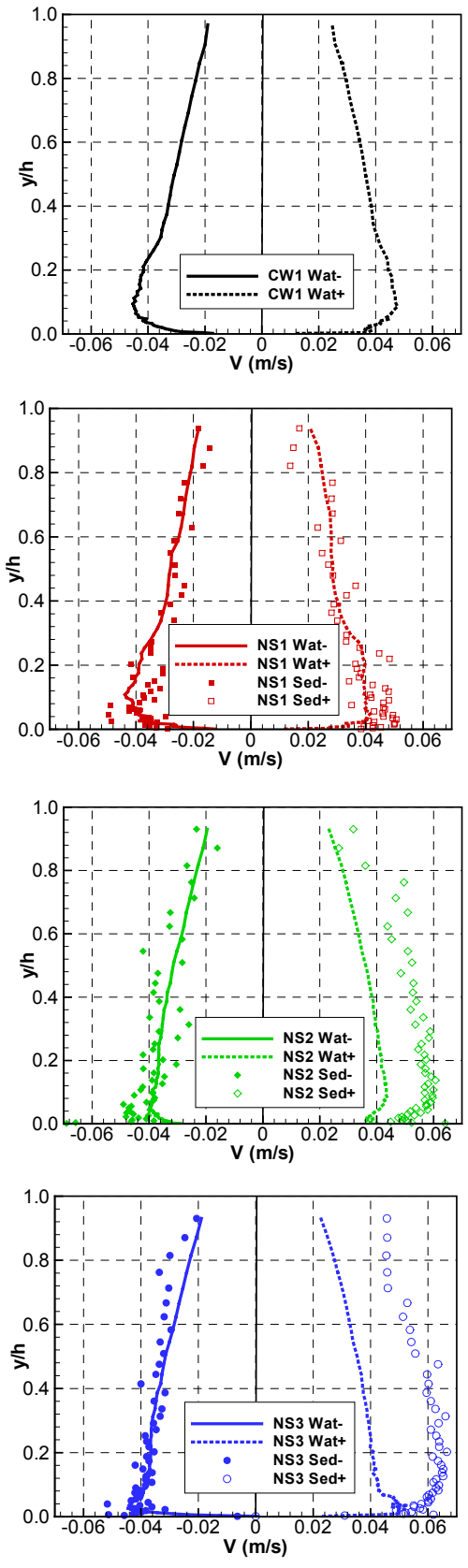

b.)

Figure 4. Vertical velocity profiles for water and sediment for the NS flow cases: a) average profiles; b) profiles split according to the upward and downward movements.

An important observation related to the profiles in Figure 4.b is that there is a wide difference between the number of measurements of upward and downward velocities in the particle samples throughout the depth (a ratio of upward/downward particle number up to 4). In contrast, the number of measurements in the water samples is almost equal throughout the depth. The high ratio of upward to downward particles in the sample confirms one of the simplest suspension mechanism in sediment-laden flows pointed out among others by Wei & Willmarth (1991) and Kiger & Pan (2002). Specifically, in a channel flow with a mean sediment concentration gradient, the upward fluid motion will transport large amounts of sediment upward compared with the downward fluid motion because of the existence of the concentration gradient. Such a suspension mechanism will eliminate the concentration gradient over time. The fact that sediment-laden flows preserve the sediment concentration distribution suggests that there should be another process which maintains the concentration gradient.

The vertical velocity distribution for water tracers and sediment particle for the neutrally-buoyant particles (NBS flow cases) are plotted in Figure 5.a showing that there is practically no difference between the two phases indicating that the neutrally buoyant sediment follow closely the velocity of the underlying flow structures. This conclusion is also supported by the vertical velocity distributions split according to the direction of movement plotted in Figure 5.b. The larger scattering of the sediment data for NBS3 test is related to the reduced number of particles that are almost uniformly distributed over the flow depth. The shape of the velocity distribution profiles is, however, similar to that of the NS experiments with a continue decrease of the velocity magnitude in the outer flow region and an abrupt decrease near the bed.

A direct implication of the vertical velocity distribution non-symmetry for the heavy particles plotted in Figure 4 would be that the net vertical flux for sediment particles is not zero, as expected from mass conservation laws for a fully developed channel flow. Wei & Willmarth (1991) showed that despite of this asymmetry, continuity is satisfied if its calculation weighs the mean upward and downward velocities with the amount of time in the data record that the velocity is positive and negative, respectively, as will be illustrated later in the paper. The current velocity measurements were sampled with a rate of 15 Hz which is much lower than that used by Wei & Willmarth (1991) and does not allow appropriate reconstruction of the time dependent velocity time series. To accommodate the low data sampling rate used in our velocity measurements, the algorithm proposed by McLaughlin & Tiedermann (1973) and extensively used in the LDV literature (e.g., Durst et al., 1981) is adopted instead.

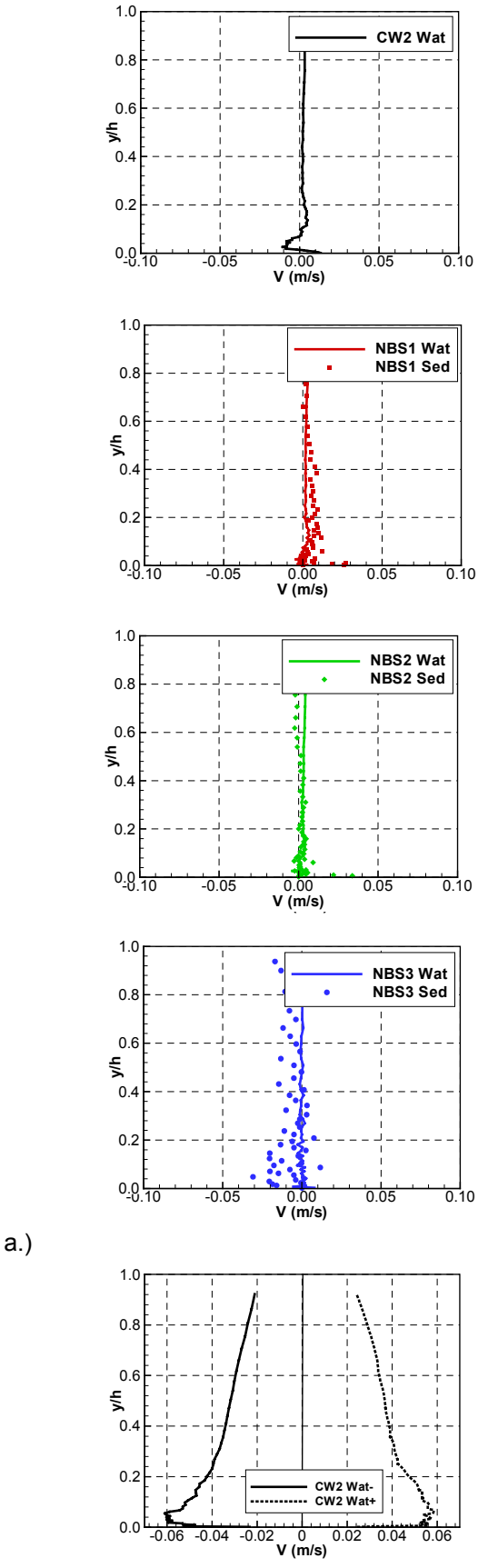

a.)

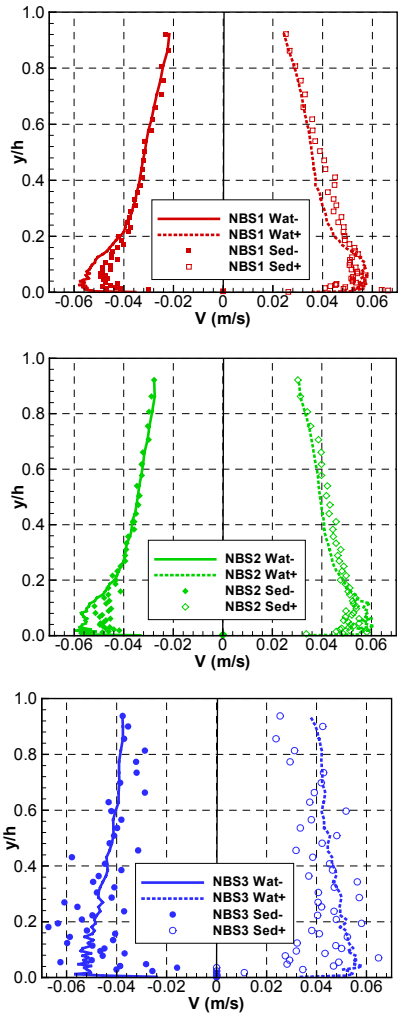

b.)

Figure 5. Vertical velocity profiles for water and sediment for the NBS flow cases: a) average profiles; b) profiles split according to the upward and downward movements.

The algorithm is formalized into the following expression:

$$V_{MLT} = \frac{1}{N}\sum_{i=1}^{N}\frac{v_i}{|v_i|} \Big/ \frac{1}{N}\sum_{i=1}^{N}\frac{1}{|v_i|} \qquad (2)$$

where the dimensionless net momentum flux is labeled as an "equivalent" velocity, V_{MLT}, with $N = N_- + N_+$ the total number of upward (N_+) and downward (N_-) data points in the sample. Equation (7) weighs the sample collected over time with the number of particles moving upward or downward. Equation (2) is plotted in Figure 6 for all NS experiments showing that continuity for the sediment fraction is fulfilled, despite the considerable asymmetry of the vertical velocity profiles for particles shown in Figure 4.

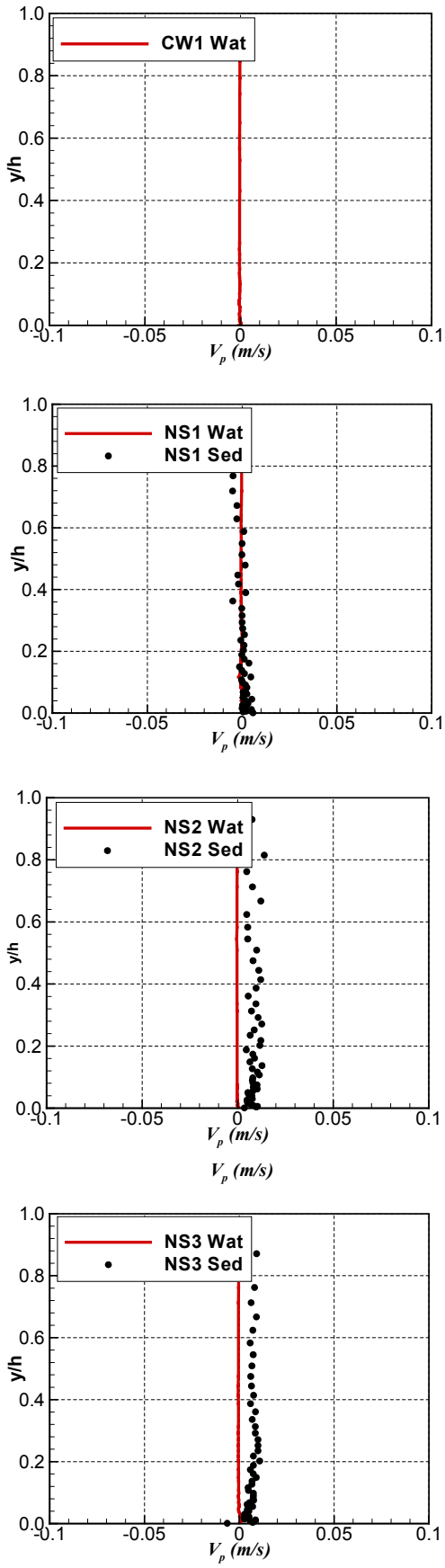

Figure 6. Distribution of vertical water and sediment particle fluxes per unit area corrected by McLaughlin & Tiederman's (1973) method

Similarly to the discussions on the horizontal velocity lag, it is reminded that there could be no velocity difference between fluid and particles in an instantaneous interaction. The velocity difference shown in the time-averaged profiles for the NS flow cases is direct representations of the effects of the particle-fluid structure interactions. Bennett et al. (1998, p. 1262) hypothesize that during the upward movement of sediment in ejections and outward interactions the relative vertical velocities of the fluid and sediment is expected to be positive and relatively high and to decrease in magnitude upwards (trends are clearly illustrated by the profiles on the left in Figure 4.b). During the downward movement of sediment the relative velocity is expected to range from positive to negative in the upper flow region and to increase negative magnitude in the lower flow regions (trends slightly confirmed by the left velocity profiles shown on the left in Figure 4.b).

When such relative velocities are averaged, the relative vertical velocities between water and sediment tend are expected to tend to zero in the upper part of the flow. Near the bed, large positive relative velocities associated with the movement of sediment in ejections are expected to be counteracted by large negative relative velocities as descending grains settle faster then the surrounding fluid. In between these regions, large positive relative velocities associated with ascending grains are expected to exceed the smaller negative relative velocities associated with the descending grains.

The mean relative velocity is never expected to attain the settling velocity in this area and the time averaged vertical velocities are always greater than the sediment particle settling velocities (the fall velocity for sediment in this experiment is 0.024 m/s). This behavior is very well captured throughout the depth by the time-averaged vertical velocity profiles shown in Figure 4.b as well as in the experiments conducted by Bennet et al. (1998). It should be mentioned that the time-averaged profiles underpredict the actual relative velocities between the sediment particles and fluid in turbulent eddies.

The horizontal and vertical mean velocity differences between fluid and particles reveal that particles in suspension tend to preferentially organize themselves relative to the flow (leading rapidly to particle cluster formation). The preferential association of a positive shift for vertical velocities with a negative shift of streamwise velocities for the particle profiles is supposedly the equivalent of the Reynolds stress turbulent correlations for the interaction between fluid structures and particles. The magnitudes of these differences are dictated by satisfying the net flux of particles in a flow situation where the mean concentration particle is constant.

1.3.3 Turbulence Intensities for Flow Phases

Turbulence modification

Turbulence modification (modulation) defines changes between the turbulence intensity of the equivalent clear water flow (which is the sediment carrier) and the water in the sediment-laden flows. The process is usually addressed in the two-phase flow community through specific relationships between characteristic time and length scales of the underlying turbulent flows (using water characteristics in the mixture) and the diameter, response time, relative velocity between sediment and water, concentration and specific gravity of the particles in suspension. Given the dilute volumetric concentrations for the flows investigated here (up to 10^{-3}) it is deemed that the particle-particle interaction is not significant and the importance of the particle-volume and mass fractions is also limited. Consequently, the relevant control parameters for the present discussion are: D_s/ℓ (ratio of the sediment size to a characteristic turbulence flow scale), Stokes number, $St = \tau_p/\tau_f$ (ratio of the particle response time to representative flow time scale), particle Reynolds number, $\mathrm{Re}_p = D_s|U - U_s|/\nu = D_s|u_L|/\nu$ (where U is the local mean streamwise velocity of water, U_s is the local mean streamwise velocity of sediment, $u_L \equiv U_s - U$ is the velocity-lag of sediment particles), particle volume and mass fractions. The physical significance of these parameters is briefly discussed below.

For D_s/ℓ < 0.1 the particles are smaller than the most energetic eddies and will follow them for at least part of its lifetime (Gore and Crowe, 1991). Fraction of the eddy energy will be transferred to the particle and turbulence intensity is thus reduced. For D_s/ℓ > 0.1 to 1, particles tend to create turbulence in its wake near the scale of the most energetic eddy, thus increasing the turbulence intensity of the fluid. In this case energy is transformed from the mean flow, which is moving the particles, to the turbulent kinetic energy of the fluid, thus overall the total energy will be decreased, as shown by the decrease of the mean bulk velocity for all flow cases. Gore & Crowe (1991) consider this ratio as being the most important parameter for turbulence modulation. The second relevant parameter controlling the turbulence modulation in these experiments is the St number related to the inertia of the particles in suspension. This particle to fluid characteristic ratio indicates that small particles (*St* << 1) will have ample time to respond to change in the flow velocity following closely turbulent eddies, while large particles (*St* >> 1) move essentially independent of the fluid. In the first case damping of turbulent fluctuations will occur, while additional turbulence will be produced in the latter case (Crowe et al., 1998). For *St* ~ 1 particles tend to centrifugate toward the peripheries of the flow structures (eddies). The last controlling parameter discussed herein, the Reynolds particle number is based on the particle size, particle-fluid relative velocity, and fluid viscosity. Particles with low Re_p cause turbulence suppression by acting as an additional source of dissipation, while particles with high Reynolds number enhance turbulence due to wake shedding (Hetsroni, 1989). Threshold value for Re_p according to Hetsroni (1989) is 400.

In the present analysis the most energetic turbulent eddies (eddies with the highest wavenumber) are associated with the Taylor scales, λ, that characterizes small eddies (microscales). This selection is based on Hinze's (1959) hypothesis that for a fully developed turbulence state, the most energetic eddies are not the largest eddies (integral scales) nor the smallest (Kolmogorov scales) where dissipation occurs. Taylor length scale sizes in between the largest and smallest length scales, hence deemed to contain the maximum kinetic energy. Taylor length scale is defined as (Tennekes and Lumley, 1972)

$$\lambda = \sqrt{\frac{15\nu\, u'^{\,2}_{rms}}{\varepsilon}} \tag{3}$$

where ε is the turbulence dissipation rate per unit mass obtained as (Nezu & Nakagawa, 1993)

$$\frac{\varepsilon h}{u_*^3} = 9.8\left(\frac{y}{h}\right)^{-0.5} \exp\left(\frac{-3y}{h}\right) \tag{4}$$

The characteristic flow time scale is defined as (Elgobashi, 1994)

$$\tau_f = \frac{\lambda}{u'_{rms}} \tag{5}$$

The particle response time is established assuming Stoke flow conditions (Kaftori et al., 1995)

$$\tau_p = \frac{1}{18\nu} D_s^2 \frac{\rho_s}{\rho_w} \tag{6}$$

where D_s is the particle diameter, ρ_s is the density of the sediment, ρ_w is the density of the water. Using Equations (5) and (6), the relationship for Stokes number becomes

$$St = \frac{\tau_p}{\tau_f} = \frac{D_s^2\, \rho_s}{18\nu\, \rho_w}\sqrt{\frac{\varepsilon}{15\nu}} \tag{7}$$

Turbulence Intensity Profiles

The plots of the turbulence intensities for mixture in the NS and NBS experiments shown in Fig. 7 (where fluid information is dominant) suggest that, overall, turbulence is affected by the presence of sediment in the near-bed region for NS experiments and throughout the depth for NBS experiments. All flow cases show an increase of streamwise and vertical turbulence intensities near the wall, for $y^+ \leq 10$.The streamwise turbulence intensities for the NS experiments

are slightly attenuated for both NS and NBS experiments in the $10 \le y^+ \le 30$ region and practically not affected for $y^+ \ge 30$, as also found by Wang & Qian (1989). A slight increase of the streamwise turbulence intensities can be observed for NBS experiments, similarly to the findings of Elata & Ippen (1961). The increase is proportional with the sediment concentration. The vertical turbulence intensities are slightly increased for the NS experiments and practically constant for NBS experiments in the $10 \le y^+ \le 30$ region. For $y^+ \ge 30$, the vertical turbulence intensities are slightly decreased for the NS experiments, while visible increased for the NBS experiments.

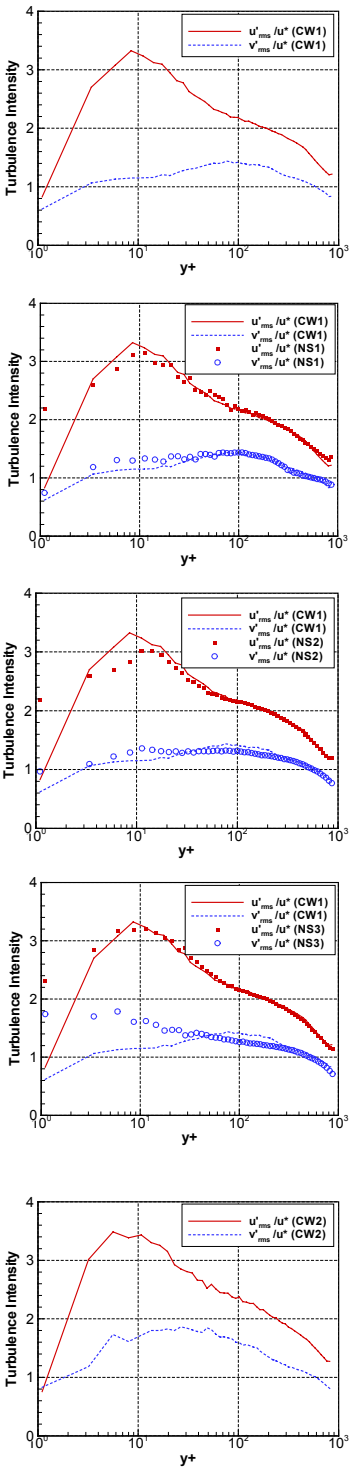

a.)

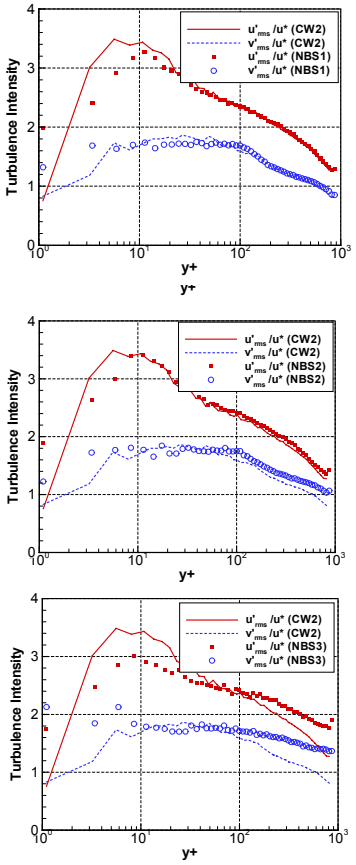

b.)

Figure 7. Turbulence intensities for the mixture: a) NS experiments; b) NBS experiments

Further insights in the turbulence modulation are provided by separately plotting the turbulence intensities for the two flow phases, as illustrated in Fig. 8. These plots reveal that for NS experiments (Fig. 8.a-c) the streamwise and vertical turbulence intensities for water are smaller in the buffer region, $10 \ge y^+ \le 30$, and are gradually larger in the inner region, $y^+ \le 10$. In the logarithmic and outer region, $y^+ > 30$, the vertical turbulence intensities decrease, obeying the damping criterion with respect to St number. The streamwise turbulence intensities in the same region show much less reduction. The streamwise velocity fluctuations trends for water are in very good agreement with those of Kiger & Pan (2002) - closest flow NS1- and Righetti & Romano (2004) – closest flow NS2 –, while for the vertical velocity fluctuations with the results of Righetti & Romano (2004). The results of Best et al. (1998) show similar, but magnified trends, due to the fact that the channel bed was covered with a layer of particles identical with those in suspension. The particle streamwise turbulence intensities are larger than those for water in the outer region ($y^+ > 30$) and smaller for $y^+ < 30$ for all cases, excepting the NS1 flow case. Particle vertical turbulence intensities are larger than those for water for all concentrations and throughout the depth.

Similar analysis for the NBS experiments (Figures 8.d-f) shows that water streamwise turbulence intensities are slightly smaller than those for clear water in the $10 \geq y^+ \leq 30$ region (log layer) and are significantly larger close to the wall for $y^+ \leq 10$. In the outer region the water streamwise turbulence intensities are increased. The water vertical turbulence intensities are larger than the clear water case for $y^+ \leq 10$, practically constant for $10 \geq y^+ \leq 30$ and increased considerably outside this region. Excepting the observed decrease of the streamwise velocity in the region $10 \geq y^+ \leq 30$, all the other trends are similar to those observed by Kaftori et al. (1998) in their study on the effect of particle presence of underlying water flow in sediment-laden flows. Rashidi et al. (1990) in experiments with neutrally-buoyant particles found that the large particles (1100 μm) indeed increase both streamwise and vertical turbulence intensities for water in the outer layer (for $y^+ > 30$), but have reverse effect for small particles (120 μm). The particle streamwise and vertical turbulence intensities for all the NBS cases are smaller than water in the $y^+ \leq 30$ region and larger outside this area. In the near wall region ($y^+ < 10$) both turbulence intensities for the particles are larger than the water ones. These observations are consistent with those made in LDV experiments for volumetric concentration of 10^{-4} by Kaftori et al. (1995.b).

Turbulence intensities for water in the mixture exceeds those for the reference clear water flow in the vicinity of the wall ($y^+ < 10$) for both heavy and neutrally-buoyant particles, as a consequence of the intense turbulence exchange between fluid and particles in this regions. Comparison of the present NS measurements with Righetti & Romano (2004) reveals that the region of significant turbulence increase near the wall is larger in their case, especially for the vertical component; the difference is associated with their larger near bed sediment concentration. Particle turbulence intensities in the present experiments are larger than those of the fluid throughout the outer region revealing a significant momentum exchange between the phases. The intensification of the momentum exchange in the area of the maximum bursting activity, i.e., $10 < y^+ < 30$, is reflected by the smaller streamwise particle turbulence intensities and the larger vertical turbulence intensities compared with the carrier phase. This intensification is considered by Righetti & Romano (2004) responsible for the reduction of the turbulent energy production in the buffer layer that might explain the turbulent damping of the fluid in the outer layer. Comparison of the present results with those obtained by Kiger & Pan (2002) and Righetti & Romano (2004) indicates higher particle vertical turbulence intensities than for water in the mixture for the $10 < y^+ < 30$ region. The difference can be associated with the increased number of particle in suspension in this area compared to both later studies.

The overall trends described above and the comparison between the NS and NBS experiments shed light on the effect of turbulence modulation in general and the role played by inertia in the process. Comparison of the NS and NBS experiments reveals, as expected, that inertia mostly affects the vertical turbulence intensities. Major differences due to inertia are is the overall increase of water the turbulence intensities in the outer region $y^+ > 30$. This trend, observed by previous similar experimental results (Kaftori et al., 1995), are not predicted by the typical St and D_s / ℓ turbulence modulation control parameters, leading to the conclusion that particle-volume and mass fractions might be also involved in the changes. Regarding the particle turbulence intensities the differences are more pronounced for the vertical turbulence intensities that are closer to those of the carrier flow for the NBS experiments.

The NS-NBS comparison should be viewed from the perspective of large near-bed sediment concentrations for the NS experiments and quasi uniform distribution of the sediment in the NS experiments. The trends summarized above are better substantiated with the increase in the sediment concentration, i.e., in general, the differences that define the trends are more visible with the increase of concentration. It is observed that the differences are practically the same for the streamwise velocity component throughout the depth and increased for the NBS compared to the NS counterparts in the outer region for the vertical turbulence intensities. The differences between the turbulence intensities of the flow phases in the mixture are better substantiated for the vertical turbulence intensities than for the streamwise turbulence intensities. For practically same underlying flow and particle concentration, size and shape this difference can be only associated with the difference in particle densities.

The present results demonstrate that modulation of turbulence requires consideration of the complex interplay of the particle-fluid interaction with the global flow characteristics. For the present results, where the D_s / ℓ and Re_p ratios were practically the same for the NS and NBS experiments, the trends in turbulence modulation would have been expected to strongly depend on the Stokes number. While trends are in agreement with Stokes number predictions for NS experiments, it does not explain the considerable water turbulence enhancement in the outer layer for the NBS experiments. Full understanding of turbulence modulation requires simultaneous consideration of the particle-fluid interaction microphysics (vortex shedding from particle wakes, particle inertia, particle-fluid structure interaction, and particle clustering) with flow the macro-level flow changes due to bed roughness and the gradients of particle concentration, flow velocities, and turbulence scales (in the absence of additional complexities induced by multisize particle in the flow).

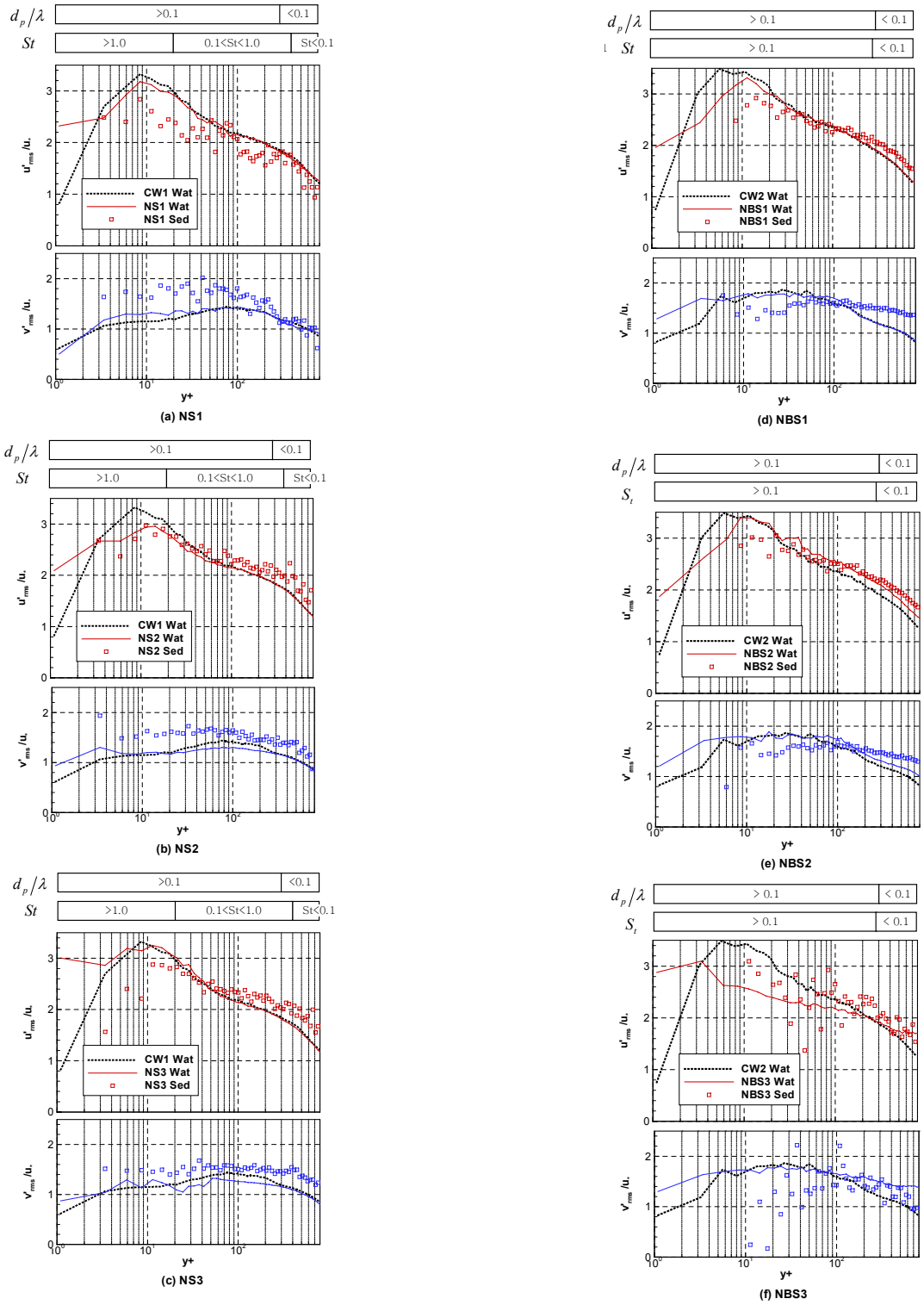

Figure 8. Turbulence intensities for the flow phases in NS and NBS experiments

1.3.4 Reynolds stresses for water in the mixture

Reynolds stress typically quantifies the turbulent shear occurring for a fluid in a given turbulent flow regime and geometry. The physical signification for sediment particles, as reported in various studies, does not have a straightforward interpretation, hence it is not reported herein. For a turbulent, fully developed open channel flow the Reynolds stress variation for the carrier fluid can be expressed as a linear function of depth for most of the flow depth excepting very close to the bed where viscous effects become dominant (White, 1991)

$$-\frac{\overline{u'v'}}{u_*^2} = \left(1 - \frac{y}{h}\right) \qquad (8)$$

Reynolds stress profiles for the NS and NBS experiments are plotted against Eq. (8) in Fig. 9.a and b, respectively. The stress distribution for all flow situations reveals that the turbulent stresses follow well the linear distribution. Small changes in the magnitude of the Reynolds stresses can be observed: a slight decrease for the NS experiments and the opposite for the NBS experiments. The stress peak increases in magnitude and its location is shifted toward the channel with the increase of sediment concentration for the NS experiments. These trends are not very clear in the plots of the stresses for the NBS cases due to the larger data scattering.

No significant changes in the Reynolds stress distribution were reported by Best et al. (1998), Graf & Cellino (2002) for similar experiments with heavy particles, while Righetti & Romano (2004) found reduced stresses compared with the clear water flow. For flows with neutrally-buoyant particles Rashidi et al. (1990) found that fairly large particles increases Reynolds stresses (volumetric concentration of 10^{-4}) while small particles reduced them. Kaftori et al. (1998) found no change near the wall and slightly reduced Reynolds stresses in the outer layer in their experiments with particle in the range 100-275 μm and volumetric concentration of 10^{-4} (similar conditions to NS1 flow case) and increased Reynolds stresses for larger particle (900 μm).

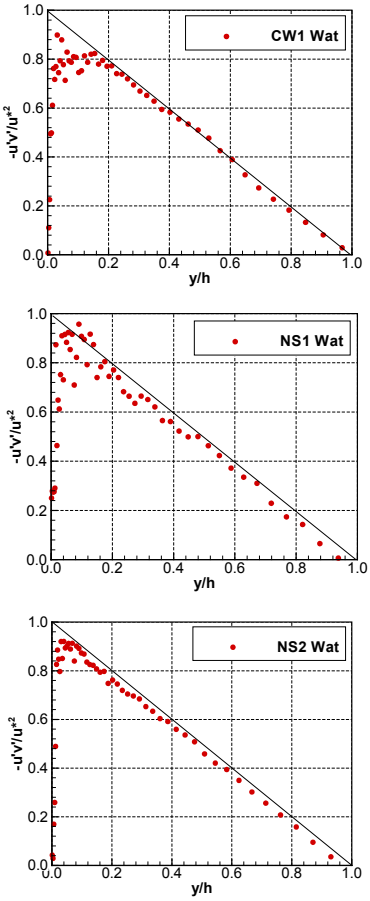

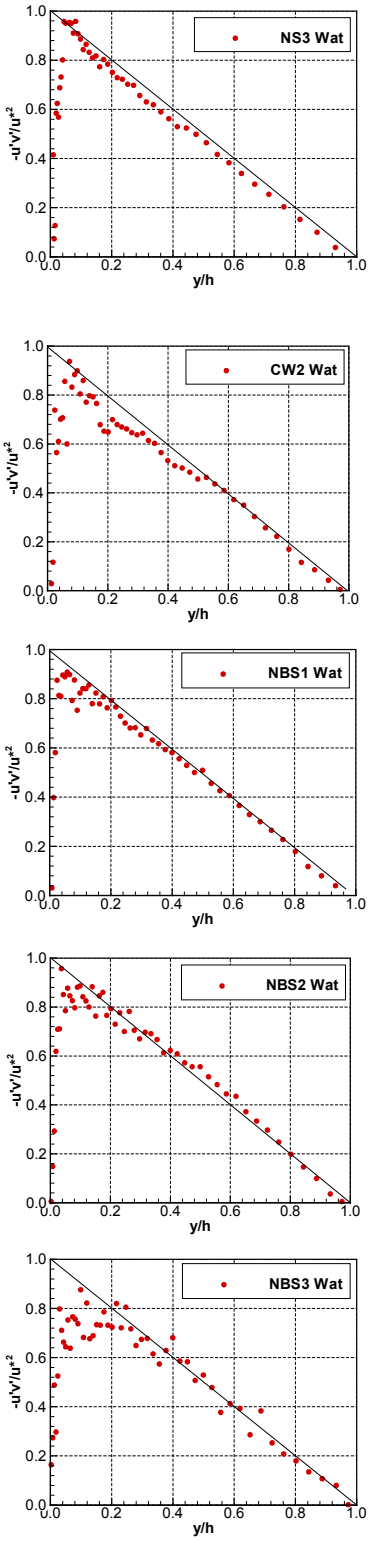

a.)

b.)

Figure 9. Reynolds stress distributions: a) NS experiments, b) NBS experiments

While there is not a clear conclusion regarding the changes in the Reynolds stress magnitude, the commonality for the available studies is its linear variation toward the bed in sediment-laden flows

justifying the use of the linear interpolation to the bed for determining the friction velocity with Equation (8).

1.3.5 Eddy viscosity for water in the mixture

The turbulent momentum diffusion coefficient (eddy viscosity), ε_m , defined as

$$\varepsilon_m = -\frac{\overline{u'v'}}{\partial U/\partial y} \qquad (9)$$

can be expressed using the log-law as (Nezu & Nakagawa, 1993)

$$\varepsilon_m = \kappa u_* h \eta (1-\eta) \qquad (10)$$

The experimentally determined momentum diffusion coefficients and Equation (10) using *k* determined from experiments are plotted in Figure 10.

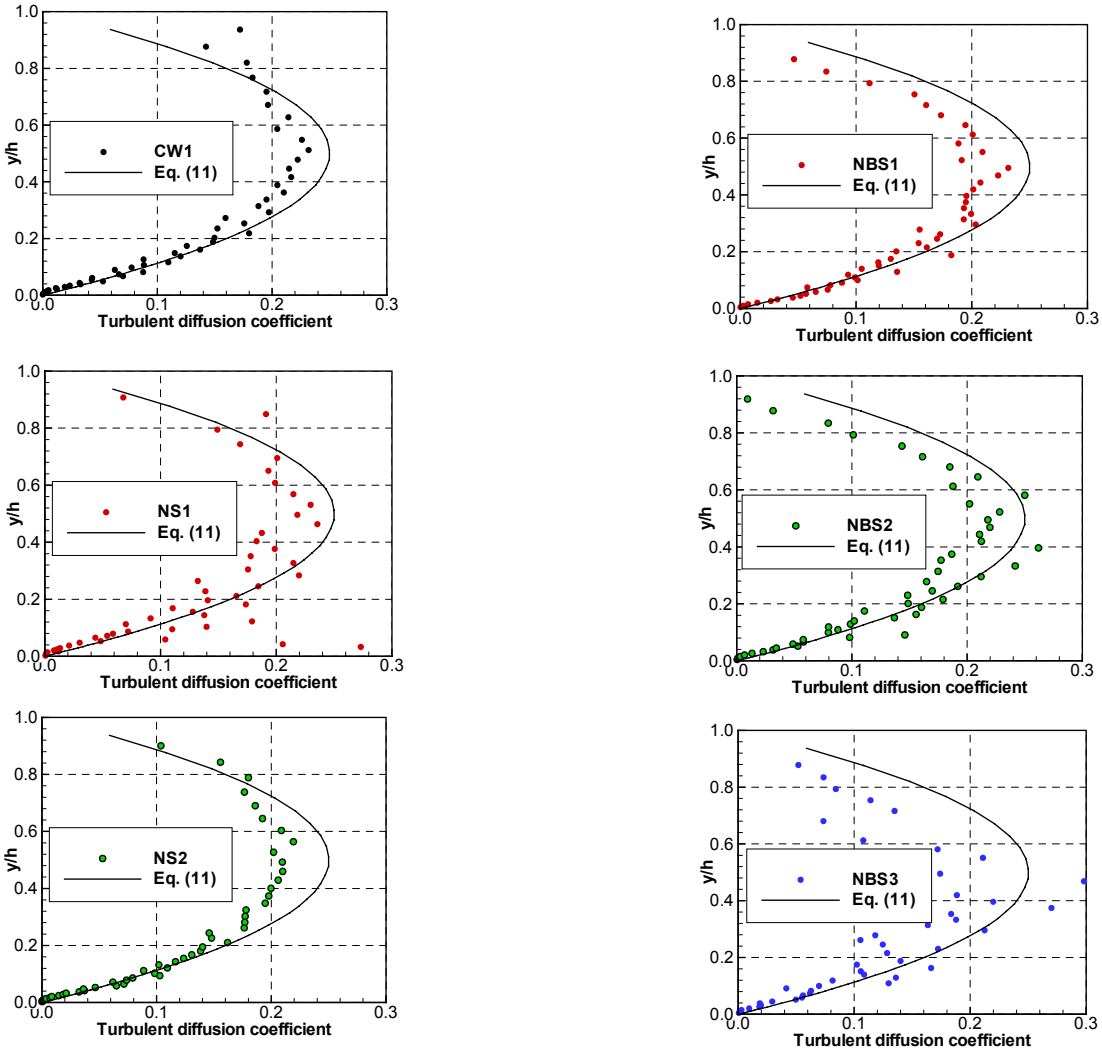

Figure 10. Turbulent diffusion coefficient distributions: a) NS experiments: b) NBS experiments

The distributions show a "quasi" parabolic distribution without a good matching of the theoretical distribution for the region $y/h > 0.3$. Differences between the measured momentum diffusion coefficients and the theoretical profile can be partially attributed changes of the water velocity profiles for water in the flows with sediment. The plots suggest that the momentum diffusion coefficient is decreased for NS and more visible for the NBS experiments. Excepting the $y/h < 0.3$ region, the trends are obscured by the data scatter. It can be noted that the scattering decreases overall for the NBS experiments compared to NS because for same bulk sediment concentrations, in the NS experiments the sediment is mostly near the bed while the NBS is well distributed over the entire flow depth, as will be shown later. Similar data quality and reduction for the momentum diffusion coefficient profiles were obtained in dilute sediment laden flows Best et al. (1997) and Graf & Cellino (2002) underlying the difficulty of these types of measurements.

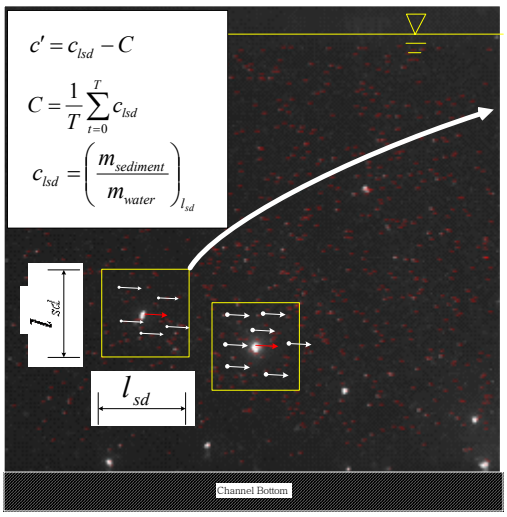

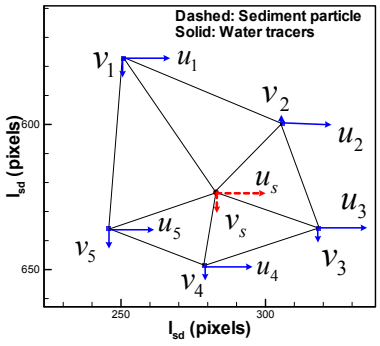

$$v' = \frac{1}{N}\sum_{n=1}^{N} v_n \qquad on \quad l_{sd} \times l_{sd}$$

$$\beta = \frac{\overline{c'v'}}{\partial C/\partial y}$$

Figure 11. Algorithm for calculation of the sediment diffusion coefficient

The addition of sediment seems to decrease the momentum diffusion coefficient for both heavy and neutrally-buoyant particles, and implicitly reduces the eddy size in the outer flow region, for $y/h > 0.3$. A decrease of momentum diffusion coefficient would imply an increase of β with the addition of sand. The questionable large values for β obtained applying Rouse test to the measured concentration data can be attributed to limitations of the Rouse equation in the $y/h > 0.3$ area. Specifically, in this region particle suspension might not be related to mean turbulence characteristics (Reynolds stress control), but with turbulent eddies with relatively greater turbulence intensities and mixing length as argued by Bennett et al. (1998) and Kiger & Pan (2002).

Sediment diffusivity coefficients could not be obtained from the existing measurements due to the limited number of recorded images and dilute sediment concentrations. With enough such raw data, a direct measurement procedure as illustrated in Fig. 11 could be employed to accurately determine this crucial parameter for suspended sediment transport. It should be additionally mentioned that this procedure also requires high water tracer concentrations in the neighborhood of the particles.

1.3.6 Sediment Concentration Profiles

PTV does not measure directly concentration, but particle number (fluxes), therefore a conversion is needed to report sediment concentrations. The volumetric sediment concentration follows a methodology developed by Bennett et al. (1998) for their Phase-Doppler Velocimetry meaurements. Assuming that the distribution of sediment particles in transverse direction is homogeneous, the area sediment particles occupy is proportional to the concentration of sediment

$$\overline{C}_{vs} \propto \frac{\text{Area of sediment particles}}{\text{Area of an image}} = \frac{\frac{\pi}{4} D_i^2 \times n}{\Delta x \Delta y} \tag{11}$$

where n is the number of sediment particles, Δx and Δy is the width and the height of sampling bin (cell), respectively. Knowing the average volumetric concentration of sediment, it is possible to introduce a coefficient, A_c , to match the left- and the right-hand side of Equation (11). Using Equation (11) and the coefficient A_c, the time-averaged sediment concentration for cell can be calculated as

$$\overline{C}_{si}(y_i) = A_c \frac{\pi D_i^2 \times n_i}{4 \Delta x \Delta y_i \times m} \tag{12}$$

where n_i is the number of sediment particles of cell i and m is the total number of image pairs.

For a steady uniform turbulent channel flow the local average concentration at elevation y in the flow, C_s is given by Rouse equation (Vanoni, 1975)

$$\frac{C_s}{C_{sa}} = \left(\frac{h-y}{y} \cdot \frac{a}{h-a} \right)^{\frac{v_s}{\beta k u_*}} \quad (13)$$

where Csa is the mean sediment concentration at a conventional elevation α. The depth-averaged coefficient β, defined as

$$\beta = \frac{\varepsilon_s}{\varepsilon_m} = \frac{1}{h-a} \int_a^h \beta(y) dy \quad (14)$$

relates sediment diffusion coefficient $\varepsilon_s = \frac{\overline{c'v'}(y)}{\partial C_s(y)/\partial y}$ and momentum diffusion coefficient $\varepsilon_m = \frac{\overline{u'v'}(y)}{\partial U(y)/\partial y}$.

Normally the sediment reference concentration is taken at $a = 0.05h$, where the top of the bed load layer is assumed. For the present cases where a distinct peak in sediment concentration was present, the maximum concentration value was taken as reference. Rouse number, z, in Eq. (13) is given by

$$z = \frac{v_s}{\beta \kappa u_*} \quad (15)$$

β is generally assumed to be 1.0. Using fall velocities determined with Dietrich's (1982) formulas, k and u^* for derived for each flow case the values of z and subsequently β were obtained sing the concentration measurements. The calculated Rouse numbers and β -values for the NS and NBS experiments are shown in Table 5. The calculated β -values are much larger than 1.0 for NS experiments and much smaller than 1 for the NBS experiments. The β values obtained for the NS experiments considerably contrast Graf & Cellino's (2002) results obtained with direct measurements of sediment diffusion coefficients and k =0.41.

Table 5. Rouse numbers and β -values for the tested flows

NS experiments			
Experiment	**NS1**	**NS2**	**NS3**
Fall velocity, v_s (m/s)	0.024	0.024	0.024
Rouse number, z	0.8	1.04	0.94
β	2.65	1.75	2.04
NBS Experiments			
Experiment	**NS1**	**NS2**	**NS3**
Fall velocity, v_s (m/s)	0.0006	0.0006	0.0006
Rouse number, z	0.07	0.07	0.19
β	0.52	0.55	0.22

Figures 12 show the profiles of sediment concentration, and the Rouse equation plotted with the parameters shown in Tables 5 for the NS and NBS experiments, respectively. Rouse equation fits well the NS data in the area 0.05< y/h <0.3, but departs from the data for the rest of the depth. Departure of the measured sediment concentrations from Rouse equation very close to the bed, y/h < 0.05 can be associated with the lack of particles on the bed in the present experiments, compared with the equilibrium sand bed (where the concentration profiles saturate) for which the equation was developed. Consequently, the location of the maximum concentration is not at the bed as predicted by Rouse's profile but at some distance from the bed (as shown in Figure 11)

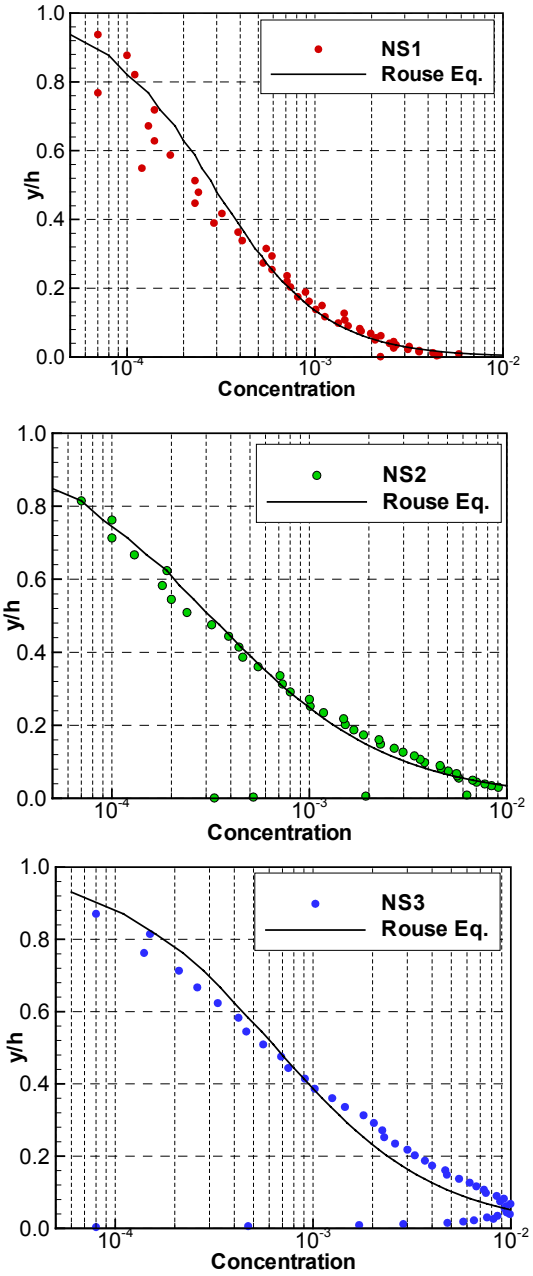

a.)

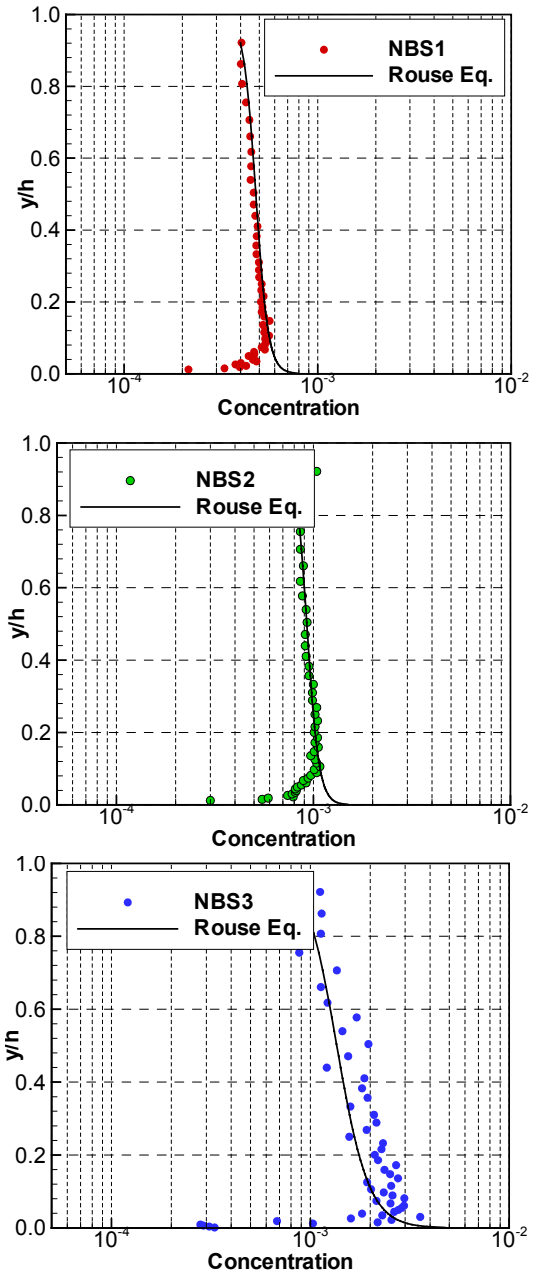

b.)

Figure 11. Sediment concentrations: a) NS experiments; b) NBS experiments

1.4 IMPLICATIONS FOR SEDIMENT TRANSPORT

1.4.1 Traditional suspended sediment transport formulation

The investigation reported targeted essential aspects of sediment transport, hence a summary of the governing equations related to this process are briefly reviewed. The main quantities of practical interest in suspended-sediment transport in alluvial channels are the average suspended concentration of sediment C_s and the total unit sediment discharge q_s. Most of the existing analytical formulations used for predicting suspended sediment transport concentration and rates are based on the single-phase (mixture) approach (e.g. Wang & Adeff, 1986; Spasojevic & Holly, 1993; Gessler et al., 1999; and Wu et al., 2000). These formulations are built the advection-diffusion equation derived from mass conservation in conjunction with a set of assumptions

$$\frac{\partial}{\partial t}(\rho_m C_s)+\frac{\partial}{\partial x}(\rho_m C_s u)+\frac{\partial}{\partial y}(\rho_m C_s v)-\frac{\partial}{\partial y}(\rho_m C_s v_s)+\frac{\partial}{\partial z}(\rho_m C_s w)$$
$$=\frac{\partial}{\partial x}\left(\varepsilon_{sx}\frac{\partial \rho_m C_s}{\partial x}\right)+\frac{\partial}{\partial y}\left(\varepsilon_{sy}\frac{\partial \rho_m C_s}{\partial y}\right)+\frac{\partial}{\partial z}\left(\varepsilon_{sz}\frac{\partial \rho_m C_s}{\partial z}\right) \quad (16)$$

where ρ_m = density of a mixture of water and sediment; $\varepsilon_{sx}, \varepsilon_{sy}, \varepsilon_{sz}$ = sediment diffusivity coefficients in x-, y-, and z-direction, respectively. The main assumptions associated with E_q. (16) are

(1) streamwise sediment particle velocity components is the same as fluid velocity

(2) sediment vertical velocity in turbulent flow is equal to the fall velocity of the sediment in still water

(3) turbulence effects of water and sediment, lumped into the diffusivity coefficients, are neglected by considering that the turbulent momentum diffusivity is equal to the sediment diffusivity.

For a steady uniform turbulent flow in a wide rectangular channel without any internal sources, integration of Equation (16) over the flow depth and additional assumptions on turbulence provides C_s via Rouse equation (Equation 13). The unit suspended sediment discharge q_s is computed from the depth-integrated advective flux of sediment C·U above the bed layer y > a

$$q_s = \int_a^h C_s \cdot U dy \quad (18)$$

The corresponding total suspended sediment discharge in the stream is obtained from integration of the unit suspended sediment discharge over the entire width of the channel. A general form for the distribution of the mean velocity, U, in sediment-laden flows accounting for the sediment concentration is given using a modified Coles' law

$$\frac{U}{u_*}=\frac{1}{k}\ln\frac{u_* y}{\nu}+B+B_r+\frac{2\Pi}{k}f\left(\frac{y}{h}\right)+X\left[C_s\left(\frac{y}{h}\right)\right] \quad (19)$$

where, k_s is the equivalent sand roughness, ν is the kinematic water velocity, B and B_r are additive constants associated with smooth rough walls, respectively, Π is the Coles' wake parameter, and

$X(C_s)$ is a parameter related to the sediment concentration profile.

1.4.2 Limitations and perspectives

Currently, all the parameters required by the traditional suspended sediment transport formulation are determined from experimental observations that are now regarded as classical flume experiments. Most of the available experimental evidence is however narrow, does not distinguish between flow phases, do not account for the role of the instantaneous interaction between flow structure and sediment particles and is often conflicting. The lack of the agreement is partially a reflection of the multiple sources of bias errors (methods, instrumentation and analytical tools) that can be involved in the experimental investigation of sediment-laden flows and (Muste, 2002).

A general limitation of the current analytical approach stems from the fact that Equation (16) has not yet appropriate experimental and/or numerical evidence to provide reliable information on the parameters controlling the microphysics of the suspended sediment process and hence to formulate closure relationships. Moreover, the results of the present study concurs with the previous findings (Squires & Eaton, 1990; Elgobashi, 1994; Kaftori et al, 1998; Rouson & Eaton, 2001) in revealing that the traditional assumptions associated with the conventional theory of suspended sediment are not accurate or quite questionable. The implications of the conceptual bias associated with the conventional theory are rarely evaluated. For example, Aziz (1996) demonstrates that the lack of consideration of the velocity lag might overestimate suspended-sediment load by up to 40%.

Use of Equations (13) and (19) encounters additional difficulties associated with the selection of proper values for β, C_{sa}, and of a velocity distribution law valid for sediment in suspension. The current methods of estimating β in Rouse equation are based on the balance of downward settling of grains and their upward diffusion in turbulent eddies (Vanoni, 1975). Many studies show that the β=1 is not justified (e.g., Jobson & Sayre, 1970; Bennett et al., 1998) without a clear agreement on its trends. Perhaps the most serious concern with the Rouse equation (Equation 13) is that the sediment diffusivity is rarely calculated directly using quantitative observations of the motion of sediment in turbulent eddies. In one of those rare attempts, Graf & Cellino (2002) determined β totally independent from the Rouse equation and found, in sharp contrast with the present results, that β <1 for suspension flow over movable bed without bedforms and small size sediment. This findings needs to be confirmed by more experimental evidence, preferably obtained with techniques allowing separate flow-phase measurements and fresh estimation approaches (see Figure 11).

Finally, there has been much controversy on the effects of sediment on the mixture streamwise velocity distributions used in Equation (19). Lyn's (2000) analysis of these semi-empirical models for velocity and concentration in flat-bed sediment-laden flows showed that models developed over the last 25 years are inadequate or at least incomplete. The above discussed limitations illustrates how tenuous is the database on which much of the computational fluid dynamics edifices of suspended sediment transport are erected.

Use of models devoid of flow structure information cannot reliably predict even first-order velocity statistics. There is no doubt that near-wall structures play a crucial role in the sediment entrainment and suspension mechanisms. Numerical studies confirmed their existence (e.g., Rouson & Eaton, 2001) and suggest that they maintain their identity in both smooth and large scale roughness (Zedler & Street, 2001). The strong three-dimensional, time-dependent nature of the bursting events and vortex structures cannot be captured using the current time-averaging approach, which is strictly valid for stationary and homogeneous turbulence. The local, time-dependent characteristics of the processes call for a combination of time, volume, and statistical (or ensemble) averaging for accurately capture the global flow patterns. According to Greimann et al. (1999), recent applications have favored phase-weighted-ensemble-averaging, because it eliminates some of the time and volume restrictions, inherent in time- and volume-averaging.

Given the intricate nature of the carrier flow and the additional complexities brought by the presence of the particles, it is obvious that the one-phase flow (mixture) hypothesis of the current predictive formulations cannot actually capture the particle-fluid, particle-particle interactions, particle-boundary interactions (that includes bed roughness effect), and the effect of the sediment on the underlying flow turbulence. Despite the close coupling between the turbulence characteristics of the flow phases, they are distinct, and a feedback mechanism relates the two phases in the flow. Consequently a fresh experimental approach using two-phase investigative tools is needed. Fortunately the new generation of non-intrusive instruments currently available is capable of separately measure flow phases, revealing the links between turbulence structures and sediment, and, importantly, the feedback of the sediment on the underlying flow.

An increased number integrated data-driven modeling using at hand experimental techniques and the best available numerical approaches are devised to further understanding and formulation of suspended sediment transport processes. Progress in computer simulation methods and kinetic-theory analyses are leading to new opportunities to obtain the equations

of motion for multiphase flows which are strongly influenced by or dominated by the disperse phase (e.g., Boivin et al., 2000, Zedler & Street, 2001). Innovative solutions specific to sediment area are emerging by modeling the fluid-particle mixture as a pseudo-fluid with modified properties which incorporates results of measurements obtained with two-phase flow investigative instruments (Cao et al., 2003; Cheng, 2004).

1.5 CONCLUDING REMARKS

In this study PIV-PTV measurements were acquired for a series of two experiments with three dilute sediment concentrations and two types of sediment to investigate the overall effects of sediment presence on the mean and turbulence flow characteristics. The experiments were conducted with all the sediment in suspension without visible streaks formed on the flume bed, hence the changes in the flow can be attributed to the interaction between sediment in suspension and flow turbulent structure. The principal conclusions drawn from this work are the following:

- Bulk flow velocity in sediment-laden flows reduces with concentration disregard of their inertial characteristics indicating extraction of energy from the mean flow due to particle presence.
- Karman constant is gradually reduced with the addition of sediment for both neutrally-buoyant and heavy particles indicating disruption of turbulence flow mechanism in the inner region.
- Mean streamwise velocities for the heavy particles lag those of the carrier flow in the outer region with up to 5% for the range of conditions of the present study due to the combined effect of the mean gradient transport and the preferential organization of the particles within the lower velocity region of the turbulent structures.
- Mean streamwise particle velocities are larger than water very close to the wall because they are not bound by viscosity shear as in the case of water.
- Mean vertical velocities for heavy particle are higher than water velocities.
- The neutrally buoyant sediment does not display any observable difference compared to the water mean velocity profiles.
- Frequency distributions of vertical turbulence intensities have positive skewness revealing a net upward momentum flux throughout the depth.
- Turbulence intensities for the carrier water flow are slightly reduced for the heavy sediment and increased for the neutrally-buoyant sediment in the region $y^+ > 30$. For $y^+ < 10$ turbulence intensities are increased for both sediment types.
- Particle turbulence intensities are larger than those of the carrier water flow for both types of sediment for $y^+ > 30$.
- The linear Reynolds stress variation is preserved in sediment-laden flows. The peak of the Reynolds stress profiles moves closer to the wall for heavy sediment and the Reynolds stresses are slightly diminished.
- Eddy viscosity for water in sediment-laden flows is the same as for water in the region $y/d < 0.3$ and smaller outside this range for both types of sediment.
- Rouse equation is valid for $y/h < 0.3$. Because of the lack of sediment in the immediate vicinity of the wall, the Rouse equation does not predict well sediment concentration for $y/h < 0.05$.

The experimental results of this study illustrate that particle presence in a turbulent channel flow affects the flow throughout the depth irrespective of their inertia. The experimental evidence also proves that use of the traditional formulations, assumptions, and models for suspended sediment transport could be part of the differences, incompleteness, and inconsistency with respect to insights into sediment effects on water flow of existing in the suspended sediment literature. Until computational resources provide full numerical simulations of flow aspects, further understanding sediment transport could be provided by systematic, highly resolved two-phase measurements targeting a sound description of the micromechanics of the suspended sediment transport. The gathered experimental evidence can assist numerical modeling in two ways. First, the experimental evidence provides databases readily usable for development and validation of complex two-phase models. Second, while new physics is gradually incorporated in the two-phase models, the same experimental evidence can be used to improve the semi-empirical correlations currently used by the hydraulic engineering community mixture-based models. The results presented in this paper serve both goals, with special emphasis on their implications on the suspended sediment transport governing equations assumption traditionally used in hydraulic engineering.

Acknowledgements

The measurements presented in the paper were conducted at Kobe University (Japan) while the first author was supported by a Japanese Society for the Promotion of Science Fellowship. This support is gratefully acknowledged.

1.6 REFERENCES

Aziz, N. M., Bhattacharya, S. K., and Prasad, S. N. (1992). "Suspended sediment concentration profiles using conservation laws." J. of Hydr. Res., 30(4), 539-554.

Bennett, S., Bridge, J. S., and Best, J. L. (1998). "Fluid and sediment dynamics of upper stage plane beds." J. of Geophysical Res., 103(C1), 1239-1274.

Best, J., Bennett, S., Bridge, J. S., and Leeder, M. (1997). "Turbulence modulation and particle velocities over flat sand beds at low transport rates." J. of Hydraulic Eng., ASCE, 123(12), 1118-1129.

Boivin, M., Simonin, O., and Squires, K. D. (2000). "On the prediction of gas-solid flows with two-way coupling using large eddy simulation." Physics of Fluids, 12(8), 2080-2090.

Bouvard, M., and Petkovic, S. (1985). "Vertical dispersion of spherical, heavy particles in turbulent open channel flow." J. of Hydraulic Res., 23(1), 5-19.

Cao, Z., Egashira, S., and Carling, P. A. (2003). "Role of suspended-sediment particle size in modifying velocity profiles in open-channel flows." Water Resources Research, 39(2), 2-1~2-15.

Cellino, M., and Graf, W. H. (1999). "Sediment-laden flow in open-channels under noncapacity and capacity conditions." J. of Hydraulic Engineering, ASCE, 125(5), 455-462.

Cheng, N-S. (2004). "Analysis of velocity lag in sediment-laden open channel flows," Journal of Hydraulic Engineering, ASCE, 130(7), 657-666.

Coleman, N. L. (1986). "Effects of suspended sediment on the open-channel velocity distribution." Water Resources Research, 22(10), 1377-1384.

Cowen, E. A., and Monismith, S. G. (1997). "A hybrid digital particle tracking technique." Experiments in Fluids, 22, 199-211.

Crowe, C. T., Sommerfeld, M., and Tsuji, Y. (1998). Multiphase flows with droplets and particles, Academic Press, London, England.

Dietrich, W. E. (1982). "Settling velocity of natural particles." Water Resources Res., 18(6), 1615-1626.

Durst, F., Melling, A., and Whitelaw, J.H. (1981). Principles and practice of laser-Doppler anemometry, 2nd Ed., Academic Press, Inc., San Diego, CA.

Einstein, H. A., and Chien, N. (1955). "Effect of heavy sediment concentration near the bed on the velocity and sediment distribution." Institute of Engineering Research, University of California, Berkeley, CA.

Elata, C., and Ippen, A. T. (1961). "The dynamics of open channel flow with suspensions of neutrally buoyant particles." Technical Report No. 45, Hydrodynamics Laboratory, Massachusetts Institute of Technology.

Elghobashi, S. (1994). "On predicting particle-laden turbulent flows." Applied Scientific Res., 52(4), 309-329.

Elghobashi, S. E., and Abou-Arab, T. W. (1983). "Two-equation turbulence model for two-phase flows." Physics of Fluids, 26(4), 931-938.

Gessler, D., Hall, B., Spasojevic, M., and Holly, F. M. J. (1999). "Application of 3D mobile bed, hydrodynamic model." J. of Hydraulic Engineering, ASCE, 225(7), 737-749.

Gore, R. A., and Crowe, C. T. (1991). "Modulation of turbulence by a dispersed phase." J. of Fluids Engineering, ASME, 113, 304-307.

Graf, W.H. and Cellino, M. (2002). "Suspension flows in open channels; experimental study," J. of Hydraulic Research, 40(4), 435-447.

Greimann, B., Muste, M., and Holly, F. M. J. (1999). "Two-phase formulation of suspended sediment transport." Journal of Hydraulic Research, 37, 479-500.

Guo, J., and Julien, P. Y. (2001). "Turbulence velocity profiles in sediment-laden flows." J. of Hydraulic Research, 39(1), 11-23.

Gyr, A., and Schmid, A. (1997). "Turbulent flows over smooth erodible sand beds in flumes." J. of Hydraulic Research, 35(4), 525-544.

Hanratty, T. J., Theofanous, T., Delhaye, J.-M., Eaton, J., McLaughlin, J., Prosperetti, A., Sundaresan, S., and Tryggvason, G. (2003). "Workshop findings." International Journal of Multiphase Flow, 29(7), 1047-1059.

Hetsroni, G. (1989). "Particles-turbulence interaction." Int. J. of Multiphase Flow, 15(5), 735-746.

Hinze J.O. (1959). Turbulence, McGraw-Hill Book Company, Inc, New York, NY.

Jobson, H. E., and Sayre, W. W. (1970). "Vertical transfer in open channel flow." J. of Hydraulic Engineering, ASCE, 96(3), 703-724.

Kaftori, D., Hetsroni, G., and Banerjee, S. (1995a). "Particle behavior in the turbulent boundary layer. I. Motion, deposition, and entrainment." Physics of Fluids, 7(5), 1095-1106.

Kaftori, D., Hetsroni, G., and Banerjee, S. (1995b). "Particle behavior in the turbulent boundary layer. II. Velocity and distribution profiles." Physics of Fluids, 7(5), 1107-1121.

Kaftori, D., Hetsroni, G., and Banerjee, S. (1998). "The effect of particles on wall turbulence." Int. J. of Multiphase Flow, 24(3), 359-386.

Kiger, K. T., and Pan, C. (2000). "PIV technique for the simultaneous measurement of dilute two-phase flows." J. of Fluid Engineering, ASME, 122, 811-818.

Kiger, K. T., and Pan, C. (2002). "Suspension and turbulence modification effects of solid particlulates on a horizontal turbulent channel flow." J. of Turbulence, 19(3), 1-21.

Kulick, J. D., Fessler, J. R., and Eaton, J. K. (1994). "Particle response and turbulence modification in fully developed channel flow." J. of Fluid Mechanics, 277, 109-134.

Lyn, D. A. (1988). "A similarity approach to turbulent sediment-laden flows in open channels." J. of Fluid Mechanics, 193, 1-26.

Lyn, D. A. (1991). "Resistance in flat-bed sediment-laden flows." J. of Hydraulic Engineering, ASCE, 117(1), 94-114.

Lyn, D. A. (2000). "Review of models for flat-bed sediment-laden flows." Proceedings of the ASCE Conference, Minneapolis, MN.

McLaughlin, D. K., and Tiederman, W. G. (1973). "Biasing correction for individual realization of laser anemometer measurements in turbulent flows." Physics of Fluids, 16(12), 2082-2088.

Muste, M. (1995). "Particle and liquid velocity measurements in sediment-laden flows with a discriminator laser-doppler velocimeter," Ph.D. dissertation, University of Iowa, Iowa City, IA.

Muste, M. (2001). "Source of bias errors in flume experiments on suspended-sediment transport." J. of Hydraulic Research, 40(6), 695-708.

Muste, M., Fujita, I., and Kruger, A. (1998). "Experimental comparison of two laser-based velocimeters for flows with alluvial sand." Experiments in Fluids, 24, 273-284.

Muste, M., and Partel, V. C. (1997). "Velocity profiles for particles and liquid in open-channel flow with suspended sediment." J. of Hydraulic Engineering, ASCE, 123(9), 742-751.

Muste, M., and Yu, K. (2002). "Advancements in sediment transport investigations using quantitative imaging techniques." Sedimentation and sediment transport, Monte Verita, Swiss.

Nezu, I., and Nakagawa, H. (1993). Turbulence in open-channel flows, A. A. Balkema, Rotterdam.

Nino, Y., and Garcia, M. H. (1996). "Experiments on particle-turbulence interactions in the near-wall region of an open channel flow: implications for sediment transport." J. of Fluid Mechanics, 326, 285-319.

Rashidi, M. G., Hetsroni, G., and Banerjee, S. (1990). "Particle-turbulence interaction in a boundary layer." Int. J. of Multiphase Flow, 16(6), 935-949.

Raudkivi, A. J. (1999). "Keynote Lecture: Loose boundary hydraulics - grey zones." River Sedimentation, Rotterdam, The Netherlands.

Righetti, M., and Romano, G. P. (2004). "Particle-fluid interactions in a plane near-wall turbulent flow." J. of Fluid Mechanics, 505, 93-121.

Rogers, C. B., and Eaton, J. (1991). "The effect of small particles on fluid turbulence in a flat-plate turbulent boundary layer in air." Physics of Fluids, A(3), 928-937.

Rouse, H. (1937). "Nomogram for the settling velocity of spheres." National Research Council, Washington, D.C.

Rouson, D. W. I., and Eaton, J. K. (2001). "On the preferential concentration of solid particlesin turbulent channel flow." Journal of Fluid Mechanics, 428, 149-169.

Sherwood, C. R., Harris, C. K., Geyer, W. R., and Butnam, B. (2003). "Toward a community coastal sediment transport modeling system: the second workshop." EOS Transactions, 83(51), 604.

Soulsby, R. L., and Wainwright, B. L. S. A. (1987). "A criterion for the effect of suspended sediment on near-bottom velocity profiles." J. of Hydraulic Research, 25(3), 341-356.

Spasojevic, M., and Holly, F. M. J. (1993). "Three-dimensional numerical simulation of mobile-bed hydrodynamics." IIHR Technical Report No. 367, Iowa Institute of Hydraulic Research, Iowa City, IA.

Squires, K. D., and Eaton, J. K. (1990). "Particle response and turbulence modification in isotropic turbulence." Physics of Fluids, 2, 1191-1203.

Sumer, B. M., and Deigaard, R. (1981). "Particle motions near the bottom in turbulent flow in open channel: Part 2." J. of Fluid Mechanics, 109, 311-337.

Sumer, B. M., and Oguz, B. (1978). "Particle motions near the bottom in turbulent flow in an open channel." J. of Fluid Mechanics, 86(part 1), 109-127.

Sundaresan, S., Eaton, J., Koch, D. L., and Ottino, J. M. (2003). "Appendix 2: Report of study group on dispersed flow." International Journal of Multiphase Flow, 29(7), 1069-1087.

Taniere, A., Oesterle, B., and Monnier, J. C. (1997). "On the behaviour of solid particles in a horizontal boundary layer with turbulence and saltation effects." Experiments in Fluids, 23(6), 463-471.

Tennekes, H. and Lumley, J.L. (1972). A first course in turbulence, MIT press, Cambridge, MA.

Tsuji, Y., and Morikawa, Y. (1982). "LDV measurements of an air-solid two-phase flow in a horizontal pipe." Journal of Fluid Mechanics, 120, 385-409.

Umeyama, M., and Gerritsen, F. (1992). "Velocity distribution in uniform sediment-laden flow." J. of Hydraulic Engineering, ASCE, 118(2), 229-245.

Vanoni, V. A. (1946). "Transportation of suspended sediment by water." Trans. of ASCE, 111, 67-133.

Vanoni, V. A. (1975). Sedimentation engineering, ASCE.

Wang, D. (2000). "On the spatial structure of low-speed streaks and particle motion in the wall region of turbulent open channel flow," Ph.D. Thesis, Tsinghua University. (in Chinese)

Wang, S. S. Y., and Adeff, S. E. (1986). "Three-Dimensional Modeling of River Sedimentation Processes." Third Int. Symp. on River Sedimentation, Univ. of Mississippi, 1496-1505.

Wang, G. Q., and Ni, J. R. (1991). "The kinetic theory for dilute solid/liquid two-phase flow." Int. J. of Multiphase Flow, 17(2), 273-281.

Wang, X., and Qian, N. (1989). "Turbulence characteristics of sediment-laden flows." J. of Hydraulic Engineering, ASCE, 115(6), 781-799.

Wei, T., and Wilmarth, W. W. (1991). "Examination of v-velocity fluctuations in a turbulent channel flow in the context of sediment transport." J. of Fluid Mechanics, 223, 241-252.

White, F. M. (1991). Viscous fluid flow, McGraw-Hill, Inc., New York, NY.

Wu, B., Wang, S. S. Y., and Jia, Y. (2000). "Nonuniform sediment transport in alluvial rivers." J. of Hydraulic Research, 38(6), 427-434.

Yarin, L. P., and Hetsroni, G. (1994). "Turbulence intensity in dilute two-phase flows - 3: The particles-turbulence interaction in dilute two-phase flow." Int. J. of Multiphase Flow, 20(1), 27-44.

Yu, K. (2004). "Particle tracking of suspended-sediment velocities in open-channel flow," Ph.D. dissertation, University of Iowa, Iowa City, Iowa.

Zedler, E. A., and Street, R. L. (2001). "Large-eddy simulation of sediment transport: currents over ripples." Journal of Hydraulic Engineering, ASCE, 127(6), 444-452.

1.7 List of symbols

a reference point for Rouse equation
C depth averaged sediment concentration
C_a sediment concentration at depth a
D_{50} median diameter of sediment particle
D_s sediment particle diameter
d_p particle diameter
d_p^+ particle diameter $\left(\equiv d_p u_* / \nu\right)$
Fr Froude number
k skewness
N total number of particles
N_+ number of upward-moving particles
N_- number of downward-moving particles
q_s total unit sediment discharge
U depth averaged streamwise velocity of water
U_m depth averaged streamwise velocity of water-sediment mixture
U_s depth averaged streamwise velocity of sediment
u_G sediment velocity lag (Greimann, et al., 1999)
u_* shear velocity
u_{*1} shear velocity obtained from the momentum balance $\left(\equiv \sqrt{gRS}\right)$
u_{*2} shear velocity obtained from the measured Reynolds stress profile
u_t root mean square of fluctuation component of streamwise velocity $\left(\equiv \sqrt{\overline{u'u'}}\right)$
V_{MLT} equivalent vertical velocity by McLaughlin and Tiederman
υ' root mean square of fluctuation component of vertical velocity $\left(\equiv \sqrt{\overline{\upsilon'\upsilon'}}\right)$
υ_s fall velocity of sediment particle
ν kinematic viscosity of water
h flow depth
y distance from the channel bottom
y^+ dimensionless distance from the channel bottom $\left(\equiv y u_* / \nu\right)$
Re Reynolds number
Re_p particle Reynolds number
ε_m turbulent momentum diffusion coefficient
St Stokes number
λ_T Taylor microscale
ξ the rate of turbulent energy dissipation
κ Karman constant
κ_m measured Karman constant of water-sediment mixture
τ_p τ_p particle response time
τ_f representative flow time scale
τ_K Kolmogorov time scale $\left(\equiv \sqrt{\nu/\xi}\right)$
ℓ_e length scale of the energy containing eddies
η dimensionless height $\left(\equiv y/h\right)$